

SLAC – PUB – 4788
November, 1988
(M)

Something New on Weak Decays of Old Mesons^{*}

H. GALIĆ

Stanford Linear Accelerator Center

Stanford University, Stanford, California, 94309

ABSTRACT

Through a special interplay of strong and weak interactions, small but significant pieces with a “wrong” flavor could be introduced into wave functions of mesons. Thus *e.g.*, not only $(u\bar{s})$ pair, but also $(u\bar{d})$ pair can be found with some probability within K^+ , *etc.* Possible importance of such “anomalous” terms in understanding of K -meson decays is discussed in a new scheme. The scheme is characterized by diagrammatic calculations of full amplitudes in long-distance environment. Two classes of models which correctly reproduce the main K -meson branching ratios and $\Delta I = 1/2$ rule are constructed. Predictive power of the scheme is then tested in a decay of a kaon into a pion and a light hyperphoton. The main idea, and both advantages and weaknesses of the proposed procedure, are thoroughly discussed.

* Work supported by the Department of Energy, contract DE – AC03 – 76SF00515.

1. Introduction

The amplitude A_{+0}^+ for $K^+ \rightarrow \pi^+\pi^0$ decay is about 20 times smaller than amplitudes for two similar K^S decay modes. Yet, almost any simple theoretical consideration would put these three amplitudes into the same range. It becomes even more obvious how small A_{+0}^+ is, when a comparison to CP violating $K^L \rightarrow \pi\pi$ decays is done. Despite the fact that CP violating phenomena are extremely rare, there is only another factor 20 difference between A_{+0}^+ and A_{+-}^L (A_{00}^L). This puts A_{+0}^+ in the middle between CP conserving and CP violating amplitudes. What causes such a suppression of $K^+ \rightarrow \pi^+\pi^0$? Is the decay really suppressed, or – on the contrary – the decay modes of short and long-lived neutral kaons are largely enhanced? It is in a way embarrassing that after so many years and efforts we still do not have a convincing and widely accepted answer. Instead, more than a dozen different approaches are competing on a market, the most popular ones not always being based on the clearest physical pictures. With so many existing models, why to propose yet another one? First, we shall see that there is still enough room for new attempts, particularly if physics is presented in simple terms, and not obstructed by technicalities or completely lost behind layers of often mutually inconsistent concepts. Secondly, a new generation of highly precise experimental data on rare K decays is going to be available soon, and in order to benefit fully from these results, by then we should have a firm control over the basic theory. How could, *e.g.*, we be sure that some seemingly unexpected result is an evidence for a new physics, and not just a consequence of imperfection of our existing models? The goal of the present article is certainly not to give an ultimate description of K physics. Rather, it represents an attempt to trace a new and perhaps promising direction in theoretical analyses. In what follows, I will present a model based on several clearly outlined assumptions, check limits of application of these ideas, and discuss what new can be learned from them. Although the model is in a way still uncompleted, I hope that this analysis will bring us closer to better understanding of an important and extremely interesting subject.

The new model is based on the following three guidelines.

- (a) Kaon physics is determined mostly by long-distance (LD) effects, while short-distance (SD) QCD can be ignored in the first approximation;
- (b) A key role in the explanation of the $\Delta I = 1/2$ rule belongs to a neutral, flavor changing $s \rightarrow d$ transition within a single quark line;
- (c) In evaluation of amplitudes only one concept and framework ought to be used. A combination of many various ideas and methods in a calculation should be avoided.

The reader will notice that the preceding assumptions are in a sharp contrast with some of the currently popular approaches^[1]. Yet, all the assumptions are firmly embedded in physics, and some of them even have a long history. Additionally, it should be recalled that we still do not fully understand the most basic $K \rightarrow \pi\pi$ data, and it might be that only a sharp turn can bring us back to the right track. The point (b) can be supported most easily. This idea stems from some analyses in the late 50's and early 60's, and has been with us since then. Its falls and rises are described in Appendix A. In spite of some alleged difficulties, $s \rightarrow d$ transitions provide the most elegant solution to the long-standing problem of hadronic K decays. Much more controversial is the subject mentioned in (a) : the role of QCD in kaon physics. Since 1974, we are witnessing attempts to explain the kaon processes by using short-distance corrected effective Hamiltonians^[2-4]. In my opinion this elegant idea really should not be utilized in analyses of weak decays of *light* hadrons. In these processes, the lack of a large mass scale makes the use of the perturbative QCD very ambiguous. Furthermore, the actual sizes of the participating objects suggest that the long-distance QCD, and not SD corrections, govern the K decays. One might argue that the heavy weak boson (W), whose exchange happens only while quarks are closely together, provides the required large scale, but this is actually not a good explanation. The large mass M_W becomes mainly consumed by the Fermi coupling constant $G_F \sim 1/M_W^2$, and the gluons accompanying the W emission are too rare (due to smallness of QCD coupling

constant at short distances) to be important. While the assumption (a) allows us to neglect SD corrections, it creates a different kind of problems. LD corrections cannot be properly summed (except maybe in simulations on gigantic lattices) and one must rely heavily on intuition in dealing with them. I will assume that all important QCD contributions are absorbed in some semi-phenomenological wave functions of mesons and corresponding *nonlocal* vertices in momentum space, and will not make use of LD or SD QCD in any other way. Finally, in (c) a program is sought in which the full amplitudes are calculated directly, avoiding the use of various reductions and extrapolations. Why not apply *e.g.* PCAC, and eliminate first some of the mesons from physical amplitudes? This is the very procedure followed in most of today's analyses: amplitudes are related to much simpler two-body matrix elements, which are then estimated by other means. However, a simultaneous use of many different concepts in a single calculation might only bring troubles. Should we really endorse a reduction process in which several of the following implements are tied together: current algebra, renormalization group equation, bag model wave functions, sum rules, spectators, lattice theories, hadronic pole diagrams, chiral models, vacuum insertions, $1/N$ expansions, and so on? None of these concepts is problematic by itself. I only do not believe that any two of them should be matched without having first a firm control over double counting and overlaps, which are unavoidably present. But usually, nothing can be done to achieve the control. The list of objections to the usual procedure is far from being exhausted. How, *e.g.*, to tolerate a great number of open and hidden parameters in a calculation in which more than one concept is used? Or, can we truly believe in extrapolations which relate off-shell matrix elements to (on-shell!) experimental data, *etc*? I would particularly like to stress the problem of factorization. Whenever an amplitude is expressed in terms of two-body matrix elements, it is implicitly assumed that LD and SD effects can be separated. In reality, this is not very likely to happen. For example, one would never describe the double slit experiment by constructing a product of probabilities of passing through separate holes, because by doing this, one would lost all the important interference effects.

In a similar way, by assuming that SD corrections are reflected only in coefficients of some operators, while LD parts are affecting solely the evaluation of matrix elements, one neglects all non-factorizable interference effects. How big an error is that? I am afraid, a fatal one! There are indications^[5] that due to an overlap between SD and LD QCD, the factorization is not possible in weak decays of light mesons. There *are* some special situations when making products of “short” and “long” will lead to a good approximation (*e.g.*, this might happen in some high-energy scattering), but generally, in low energy kaon decays the factorization can hardly be justified.

With all the above in mind, not too much freedom was left for the construction of the new scheme. The closest to the requirements was a diagrammatic calculation based on effective meson-quark interactions. The most remarkable feature of the new model are “anomalous” vertices, with unusual flavor content. They are a result of $s \rightarrow d$ transitions happening *inside* the light mesons, and follow naturally from the assumptions (a) – (c). Both “regular” and “anomalous” vertices will be constructed and discussed in Section 2. Rules for evaluation of diagrams and amplitudes, together with an example, will be given in Section 3. Sections 4 and 5, contain a brief review of the most important results. (More detailed study of the main K decay modes will be presented elsewhere). The concluding section is devoted to a critical examination of the proposed model. The role which $s \rightarrow d$ transitions have played in explanations of K decays is reviewed in Appendix A. Another model (“Model B”) for anomalous vertices is presented in Appendix B.

Throughout the work the four-flavor version of the standard model is used, but a generalization to more flavors presents no problem. The notation closely follows an earlier work^[6] on the subject. (See also Refs. 7 and 8).

2. Model

In this section, the attention will be focused on the relationship between light mesons and their constituents. The final goal will be a construction of semi-phenomenological meson – quark couplings, which later will serve in diagrammatic calculations of various processes. A diagrammatic approach to K decays was attempted earlier by Pascual and Tarrach^[9]. There are however differences between Ref. 9 and the present work. In Ref. 9, *e.g.*, only local meson – quark vertices were used, while here the vertices will be non-local. More recently, Gilmour^[10] has also presented a diagrammatic study of hadronic weak decays, but in a nonrelativistic framework. Here, I will develop a fully relativistic picture.

Imagine the existence of a probe capable of determining the flavors and four-momenta of quarks within a meson, at a certain time. If the valence quarks approximation is not too misleading, we would observe fractions $q_1 = k + P/2$ and $q_2 = -k + P/2$ of the total meson momentum P^μ , carried away by quark and antiquark respectively (see Fig. 1). We would also be able to plot a probability distribution $H(k, P)$, for finding a combination of quarks with relative momentum $q_1 - q_2 = 2k$ within the meson. The probability distributions will in turn be related to wave functions of the mesons, and *vice versa*.

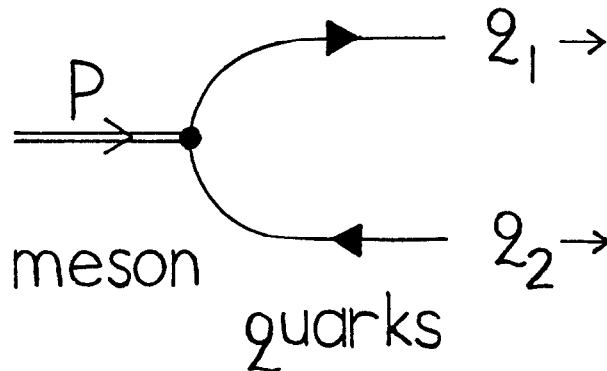


Fig. 1. Quark content of a meson in the valence approximation. The momentum of the antiquark is $q_2 = P - q_1$.

Unfortunately, such a miraculous probe does not exist. Yet, on basis of rather

general arguments, one can *construct* the distributions $H(k, P)$, and test them indirectly in analyses of decay and scattering processes. An attempt of such a construction of the effective meson – quark couplings will be described in the remainder of this section.

I will begin with the assumption that the distribution $H_{\mathcal{M}}(k, P)$ for the meson \mathcal{M} is proportional to $1/(k^2 - \alpha_{\mathcal{M}}P^2)^n$. The parameter $\alpha_{\mathcal{M}}$ – as we shall see – has the value related to the weak decay constant $f_{\mathcal{M}}$ of the particular meson. For all the mesons considered in our study, the relation $\alpha_{\mathcal{M}} > 1/4$ is satisfied. The integer n is a free parameter. The above choice of $H_{\mathcal{M}}$ can most easily be understood in the rest system of a meson. The four-momenta of quarks are then reduced to $q_1^\mu = (xM, \vec{q})$, $q_2^\mu = ([1-x]M, -\vec{q})$, where x is a number between 0 and 1, and M stands for the mass of the meson. When the above momenta are substituted in the assumed expression for $H_{\mathcal{M}}$, the resulting probability distribution peaks for values of x near to $1/2$, *i.e.*, when the available energy is shared uniformly between the quarks. Similarly, the probability is higher for the smaller values of the relative momentum $|\vec{q}|$. Situations less likely to occur are, according to the proposed form of $H_{\mathcal{M}}$, those in which the relative (three-) momentum is large, or when the energy is consumed mainly by one of the quarks. This picture is in harmony with a common sense description of mesons. An asymmetry in x would probably improve the agreement with experiments. It might be introduced by adding a $k \cdot P$ piece into denominator of $H_{\mathcal{M}}$, but for sake of simplicity I will not do that. Needless to say, the presented choice is by no means unique, and devoted model builders are encouraged to find and test different functional forms.

The determination of the probability distribution is not yet completed. The proper Lorentz structure must be introduced. For pseudo-scalar mesons, this could be achieved by putting $\not{P}\gamma_5$ term in the numerator. The normalized distribution now assumes a form of a matrix,

$$H_{\mathcal{M}}(k, P) = \beta_{\mathcal{M}} M_{\mathcal{M}}^{2n-3} \frac{\not{P}\gamma_5}{(k^2 - \alpha_{\mathcal{M}}P^2)^n} , \quad (1)$$

where β is a dimensionless normalization constant. (More on α and β in the next

section. See also Ref. 6). It remains to add the confinement into the model. This is not an easy task. I will assume a zero probability for finding free, on-shell quarks in a meson. In other words, I want a decay of the meson into a pair of free quarks to be absolutely forbidden. This will be accomplished by sandwiching $H_{\mathcal{M}}$ between $(\not{k} + \not{P}/2 - m_1)$ and $(\not{k} - \not{P}/2 - m_2)$, where $m_1(m_2)$ denote the current masses of quarks which are attached to the meson. Then, it is the equation of motion, that prevents the unwanted decay to free quarks. The resulting expression, the nonlocal vertex^[6]

$$\Gamma_{\mathcal{M}}^{ij}(k, P) = \delta^{ij} (\not{k} + \frac{\not{P}}{2} - m_1) H_{\mathcal{M}}(k, P) (\not{k} - \frac{\not{P}}{2} - m_2) \quad , \quad (2)$$

will be used in a diagrammatic description of mesons, and weak processes in which mesons participate. Superscripts i, j in (2) denote colors, and δ^{ij} reflects the color conservation. The effective vertex Γ contains implicitly all the interactions between quarks to the moment of contact with our capable “probe”. Gluons hidden in the vertex are responsible for the nonlocal structure of Γ . The situation is symbolically described in Fig. 2.

How and where to use the effective vertices? An illustration of the concept might be in place here. Consider $\pi^+ \rightarrow \bar{\ell}\nu$ decay. To obtain the nonleptonic part of the amplitude (see Fig. 3), we should first multiply the probability of finding u and \bar{d} quarks with relative momentum k , by the probability that these quarks meet and form a W meson. Next, contributions of all possible relative momenta must be summed up. As a consequence, the amplitude contains an integral

$$\int d^4k \text{Tr} \left\{ \gamma_\mu (1 - \gamma_5) \frac{i}{\not{k} + \not{P}/2 - m_u} \Gamma_{\pi}^{jj}(k, P) \frac{i}{\not{k} - \not{P}/2 - m_d} \right\} \quad . \quad (3)$$

Note that Feynman propagators of u and d quarks will cancel similar factors in Γ . After the cancellation, the integral in (3) can be easily evaluated, and a straightforward calculation leads to the amplitude. We shall return to this example in the next section.

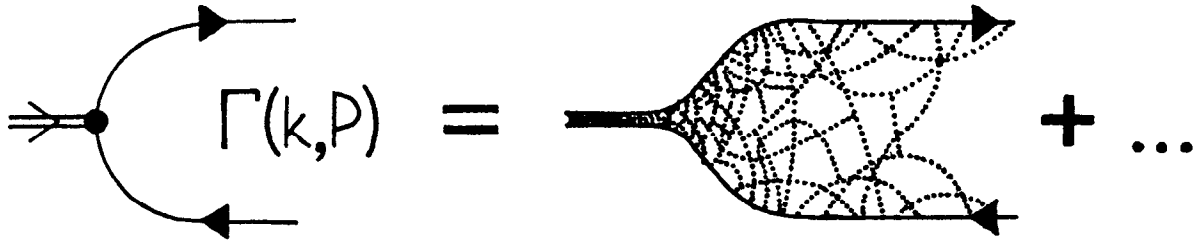


Fig. 2. Nonlocal, effective coupling of quarks to a meson.

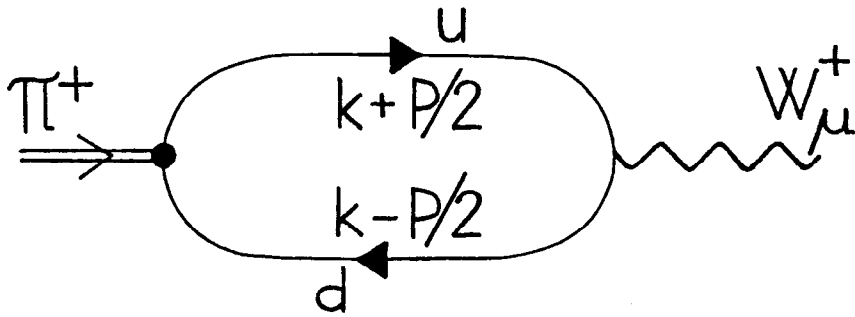


Fig. 3. Hadronic part of $\pi^+ \rightarrow \bar{\ell}\nu$ decay. P is the momentum of the pion, k the loop momentum.

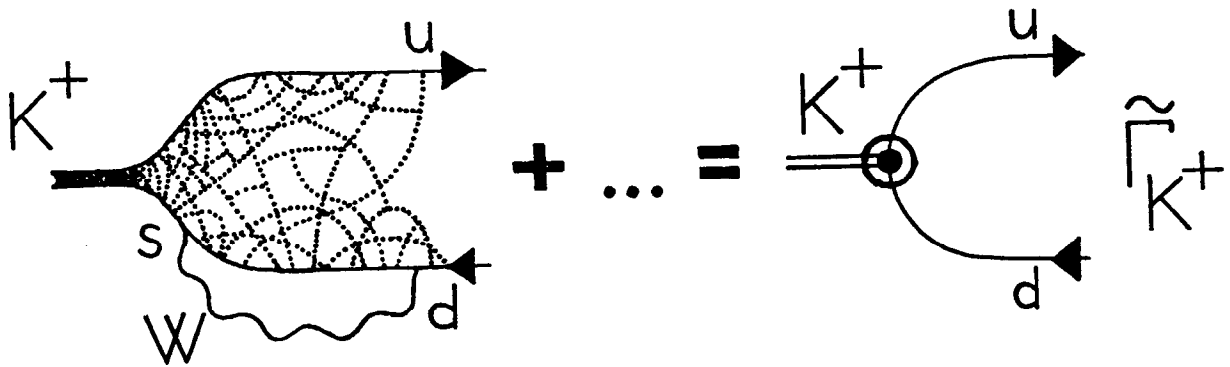


Fig. 4. Substructure of an "anomalous" vertex.

Until now, the flavor of quarks was mostly ignored. It was implicitly assumed that *e.g.*, in the case of K^+ meson, the probe would reveal a presence of u quark and s antiquark, with the probability equal to one. However, weak interactions can change the situation. Consider the diagram in Fig. 4. If W boson is captured by the same quark line by which it was emitted, the probe will detect \bar{d} instead of \bar{s} ! What is the probability for such a flavor changing transformation within a line? Without the gluons, for bare quarks, the process is down by $1/M_W^4$, and thus practically unobservable. Miraculously, gluons (and this is true for both “self-energy” gluons, and those exchanged between two different quark lines) act as a catalyst, and in their presence the probability for $s \rightarrow d$ transition gets increased to much more comfortable $1/M_W^2$. Therefore, the probability distribution $\tilde{H}(k, P)$ for finding a quark with the “wrong” flavor in a meson, is of the order G_{Fsc} , where s and c denote the Cabibbo angles ($s \equiv \sin \theta_C, c \equiv \cos \theta_C$). In many processes this will still be invisible, but — as we shall see — in certain situations even such a small contribution becomes very important. For example, the probability of forming $\bar{d}d$ pair in K^S is small, but once the pair is formed, the meson can decay very quickly through a fast, flavor conserving process. The smallness of \tilde{H} is thus in some cases counterbalanced by an increased likelihood of the subsequent strong-like subprocess.

The functional form of $\tilde{H}(k, P)$ can only be guessed. In order to keep the analysis as simple as possible, I will again assume the probability distribution in the form of an inverse power of $(k^2 - \alpha P^2)$. Guided by some one-loop arguments, I am proposing the following expressions for the distribution \tilde{H} , and the “anomalous” (named so, because of the presence of the “wrong” flavor) vertex function $\tilde{\Gamma}$:

$$\tilde{H}_{\mathcal{M}}(k, P) = \frac{G_{\text{Fsc}}}{\sqrt{2}} \beta_{\mathcal{M}} M_{\mathcal{M}}^{2n-1} Q^2 \frac{\not{P}(X + Y\gamma_5)}{(k^2 - \alpha_{\mathcal{M}}P^2)^{n+1}}, \quad (4)$$

$$\tilde{\Gamma}_{\mathcal{M}}^{ij}(k, P) = \delta^{ij} (\not{k} + \frac{\not{P}}{2} - m') \tilde{H}_{\mathcal{M}}(k, P) (\not{k} - \frac{\not{P}}{2} - m'') \quad (5)$$

Here, Q^2 denotes square of the momentum in the line in which $s \rightarrow d$ transition occurs (Q is either $k - P/2$ or $k + P/2$). α and β are the parameters already

defined in “regular” functions (1) and (2). The numerator in $\tilde{H}(k, P)$ contains the $(X + Y\gamma_5)$ matrix with mixed chirality. This is a consequence of the violation of parity in the weak transitions. The model does not predict magnitudes of X and Y , and they should be determined experimentally. For simplicity, I will assume that X and Y do not depend on \mathcal{M} . It is interesting that in some processes only X contributes (*e.g.*, in $K \rightarrow \pi\pi$), while in other decays Y is important (*e.g.*, in $K \rightarrow \pi + \gamma_Y$, where γ_Y denotes a hyperphoton), or a combination of both appears (*e.g.*, in $K \rightarrow \pi\bar{\nu}\nu$). As a consequence, it will, *e.g.*, be impossible to relate directly $K \rightarrow \pi\pi$ and $K \rightarrow \pi\gamma_Y$ decays, without introducing further assumptions. We shall return to this problem in Section 5.

Not only that the flavor and chiral structure of the anomalous vertices is unusual, there is also an important characteristic related to isospin. Since in the direct $s \rightarrow d$ transition the isospin is changed by only 1/2 unit, the anomalous vertices can not contribute to $\Delta I = 3/2$ processes^[11]. In other words, in the analysis of *e.g.*, $K^+ \rightarrow \pi^+\pi^0$ (which is a pure $\Delta I = 3/2$ decay), all diagrams with anomalous vertices should exactly cancel. This clearly provides a mechanism for a successful description of $\Delta I = 1/2$ rule. Namely, the hadronic K^\pm decays will be influenced by regular vertices only, and – as a rule – the regular vertices produce small amplitudes. On the other hand, the amplitudes A^S will mainly depend on the magnitude of X . Large X will produce big A^S , but will not in any way spoil A^\pm amplitudes. A detailed presentation of the mechanism can be found in the next section.

Finally, in order to get some control over the model-dependency, I have constructed another anomalous probability distribution. It is presented in the Appendix B. The expressions (4) and (5) in this section will be referred to as “Model A”, and the alternative model from the appendix will be called “Model B”.

3. Rules

In this section we shall consider how the effective vertices can be put to work in a diagrammatic calculation of light meson decays. One must first construct all possible (lowest order) Feynman diagrams of a process, using quark, lepton and electroweak boson lines. Gluons, according to the scheme, should be neglected. Instead, new quark – meson vertices (both regular and anomalous) should be used to close quark lines. Mesons are always on-shell, external particles, and can not be used as intermediate states. In closed fermion loops a summation over Fermi and color degrees of freedom must be performed. Accordingly, a trace calculation and the factor (-3) will accompany every quark loop (the negative sign in the factor is a consequence of the Fermi statistics). Elementary particles (quarks, leptons, ...) and point-like electroweak interactions are described by the usual Feynman propagators and vertices. The nonlocal effective vertices should be described following the general rules derived in the preceding section. In order to accommodate various symmetries and the fact that mesons can be both ingoing and outgoing objects, some additional refinement will be needed. *E.g.*, formulae (2) and (5) correspond to the situation when an incoming meson decays into two quarks, but in some diagrams we shall also need to know the probability for forming an outgoing meson out of two quarks. Furthermore, a distinction between mesons forming an isotriplet, isodoublet, or isosinglet, should be visible in effective vertices. The complete expressions for the vertices, given below, are therefore slightly different from the expressions derived in Section 2.

The regular meson – quark – antiquark vertices will be denoted in diagrams by heavy dots (see Fig. 5). Whenever an *ingoing* meson is encountered, the vertex function $\Gamma_{\mathcal{M}}^{ij}(k, +P)$ should be inserted in the formula for the amplitude; when a meson in a diagram is *outgoing*, introduce $\Gamma_{\mathcal{M}}^{ij}(k, -P)$. Here,

$$\Gamma_{\mathcal{M}}^{ij}(k, \pm P) = \pm \lambda \delta^{ij} \left(\not{k} \pm \frac{\not{P}}{2} - m_q \right) H_{\mathcal{M}}(k, P) \left(\not{k} \mp \frac{\not{P}}{2} - m_{q'} \right) . \quad (6)$$

The probability function $H_{\mathcal{M}}(k, P)$ is given by Eq. (1). λ is the Clebsch–Gordan

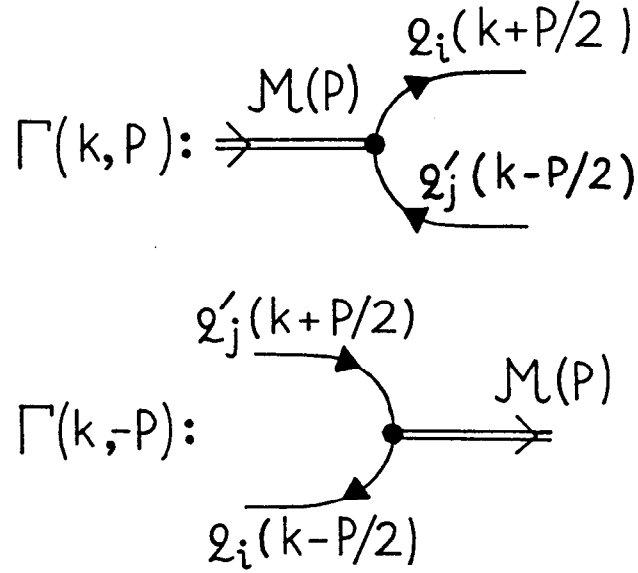


Fig. 5. Regular vertices for ingoing and outgoing mesons. (For anomalous vertices, replace $\Gamma \rightarrow \tilde{\Gamma}$, and encircle the heavy dot).

(CG) coefficient, with the value $+1$ for K^\pm, π^\pm vertices, $+1/\sqrt{2}$ for $\pi^0(\bar{u}u)$, $K^L(\bar{d}s)$, $K^L(\bar{s}d)$ and $K^S(\bar{d}s)$ vertices, $-1/\sqrt{2}$ for $\pi^0(\bar{d}d)$ and $K^S(\bar{s}d)$ vertices, etc. Constants $\alpha_\pi, \alpha_K, \dots$, in H_M could be related to values of weak decay constants f_π, f_K, \dots , while $\beta_\pi, \beta_K, \dots$, properly normalize the wave functions. One finds^[6]

$$\alpha_M = \pi (f_M/M_M) \sqrt{\frac{(n-1)(n-2)^2}{6(2n-1)}} \quad , \quad (7)$$

$$\beta_M = 4\pi \alpha_M^{n-1} \sqrt{(2n-1)(2n-2)/3} \quad . \quad (8)$$

The anomalous vertices will be denoted by encircled heavy dots (see Fig. 6). As discussed earlier, these vertices are a result of $s \rightarrow d$ (or $d \rightarrow s$) weak transitions within a meson. Therefore, in an anomalous vertex, a d quark will be attached where an s quark appears in the corresponding regular vertex, and *vice versa*: an s quark instead of the regular d quark. *E.g.*, while the flavor structure of regular vertices can be $K^+(\bar{s}u)$ and $\pi^0(\bar{d}d)$, the anomalous vertices will be $K^+(\bar{d}u)$, $\pi^0(\bar{s}d)$

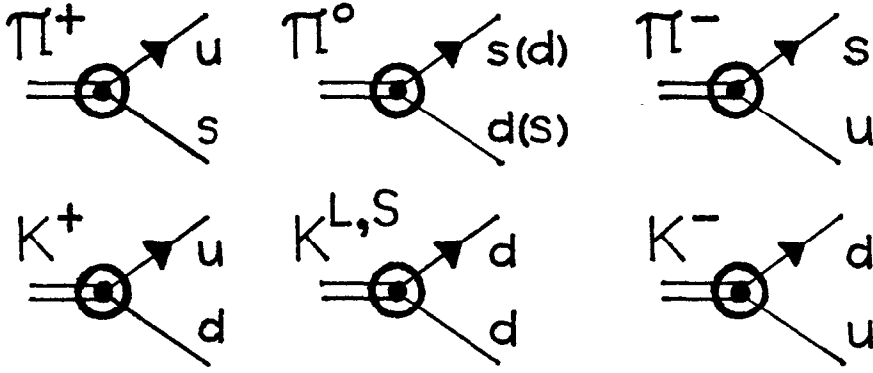


Fig. 6. Anomalous vertices for light ingoing mesons.

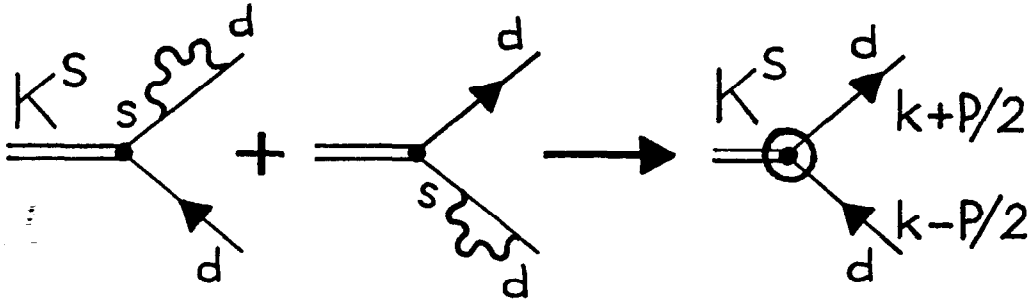


Fig. 7. Substructure of the anomalous $K^S(\bar{d}d)$ vertex.

and $\pi^0(\bar{d}s)$. The complete anomalous vertex functions are

$$\tilde{\Gamma}_{\mathcal{M}}^{ij}(k, \pm P) = \pm \lambda \delta^{ij} \left(\not{k} \pm \frac{\not{P}}{2} - m \right) \tilde{H}_{\mathcal{M}}(k, P) \left(\not{k} \mp \frac{\not{P}}{2} - m' \right) \quad (9)$$

Momenta of particles are assumed to be the same as in Fig. 5. The conventions for (\pm) signs, and CG coefficients λ , are the same as in formula (6). The probability distribution $\tilde{H}_{\mathcal{M}}(k, P)$ is defined in Section 2, Eq. (4), and contains the square of momentum of the quark line in which the flavor is changed. In π^0, K^L and K^S , such a transmutation can happen in both quark lines. Therefore, *e.g.*, the full anomalous vertex $K^S(\bar{d}d)$ contains a factor (compare to Fig. 7)

$$\lambda \tilde{H}_S \sim \frac{1}{\sqrt{2}} \left(k + \frac{P}{2} \right)^2 - \frac{1}{\sqrt{2}} \left(k - \frac{P}{2} \right)^2 \quad (10)$$

The first term originates from the $s \rightarrow d$ transition in the upper line of the regular $K^S(\bar{d}s)$ vertex, and the second term is related to $\bar{s} \rightarrow \bar{d}$ transition in the lower quark line of $K^S(\bar{s}d)$ (Fig. 7). Factors $\pm 1/\sqrt{2}$ are the CG coefficients. (For the $K^L(\bar{d}d)$ vertex, both terms in the analogous expression would be positive, because of different CG coefficients).

We can now return to the example mentioned in Section 2, namely the $\pi^+ \rightarrow \bar{\ell}\nu$ decay. To the lowest order in weak interactions the decay is represented by the diagram in Fig. 8, and the amplitude becomes (compare to Eq. (3))

$$A = \left(\frac{ig}{2\sqrt{2}} \right)^2 \bar{u}_\nu(t) \gamma^\mu (1 - \gamma_5) v_\ell(r) \frac{-i}{P^2 - M_W^2} (-3) i^2 \int \frac{d^4 k}{(2\pi)^4} \text{Tr} \left\{ c \gamma_\mu (1 - \gamma_5) \left[\beta_\pi M_\pi^{2n-3} \frac{\not{P} \gamma_5}{(k^2 - \alpha_\pi P^2)^n} \right] \right\} . \quad (11)$$

Here, $(i)^2$ in front of the integral is a remnant of the two quark propagators, and c denotes the cosine of the Cabibbo angle. The integral can be easily calculated, and with definitions (7) and (8) for $\alpha_{\mathcal{M}}$ and $\beta_{\mathcal{M}}$, one obtains

$$\begin{aligned} & (-3) i^2 \int \frac{d^4 k}{(2\pi)^4} \text{Tr} \left\{ \dots \right\} \\ &= \frac{3c}{4\pi^4} \beta_\pi M_\pi^{2n-3} \int \frac{d^4 k P^\mu}{(k^2 - \alpha_\pi M_\pi^2)^n} = (-)^n i c f_\pi P^\mu . \end{aligned} \quad (12)$$

The amplitude (11) now gets the familiar form (Note: $g^2/8M_W^2 = G_F/\sqrt{2}$),

$$A = (-)^{n+1} \frac{G_F c}{\sqrt{2}} f_\pi \bar{u}_\nu(t) \not{P} (1 + \gamma_5) v_\ell(r) . \quad (13)$$

This is no surprise, since the relation (7) between $\alpha_{\mathcal{M}}$ and $f_{\mathcal{M}}$ was determined just in a study of $\mathcal{M}_{\ell 2}$ decays.

Also contributing to the process is a diagram (Fig. 9) with an anomalous vertex, but this diagram is very suppressed. The hadronic part of the corresponding

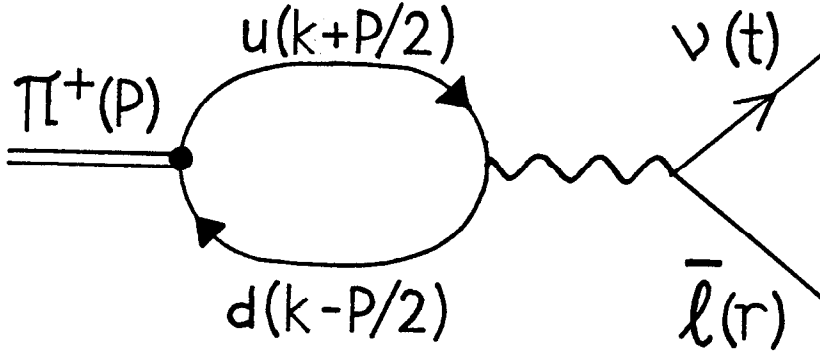


Fig. 8. The regular contribution to $\pi^+ \rightarrow \bar{l}\nu$ decay ($P = t + r$).

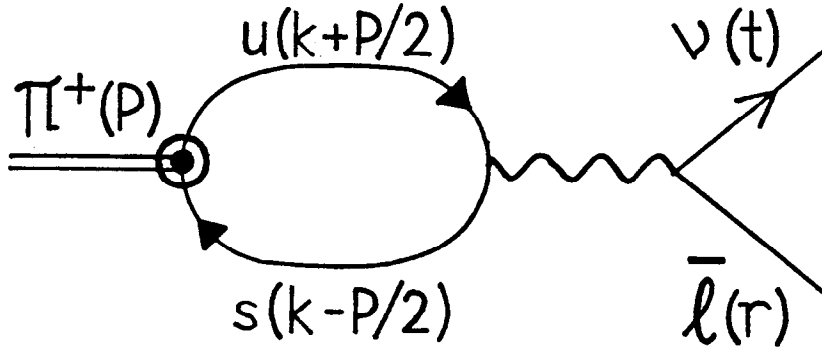


Fig. 9. The anomalous contribution to $\pi^+ \rightarrow \bar{l}\nu$ decay.

amplitude A_{ANOM} is

$$\begin{aligned}
 & (-3) i^2 \int \frac{d^4 k}{(2\pi)^4} \text{Tr} \left\{ s \gamma_\mu (1 - \gamma_5) \left[\frac{G_{FSC}}{\sqrt{2}} \beta_\pi M_\pi^{2n-1} \left(k - \frac{P}{2}\right)^2 \frac{\not{P}(X + Y \gamma_5)}{(k^2 - \alpha_\pi P^2)^{n+1}} \right] \right\} \\
 & = (-)^n i c f_\pi P^\mu \left[\frac{G_{FS}^2}{\sqrt{2}} M_\pi^2 (X + Y) \left(\frac{2}{n} - \frac{n-2}{4n\alpha_\pi} \right) \right].
 \end{aligned} \tag{14}$$

Since $G_F M_\pi^2 \sim 10^{-7}$, $s^2 \equiv \sin^2 \theta_C \sim 10^{-2}$, and $(X + Y)$ is of order $\mathcal{O}(1)$ (see the next section), the anomalous contribution is many orders of magnitude smaller than the regular one in the expression (12). Consequently, the anomalous diagram can safely be ignored in this decay. In the similar $K_{\ell 2}$ decay, the ratio A_{ANOM}/A is slightly larger ($\sim 10^{-6}$), but still negligible. In some other decays the situation will be identical: the anomalous vertex, due to a hidden $s \rightarrow d$ transition adds a second weak interaction, and the related ‘‘anomalous’’ amplitude becomes much

smaller than the first order (in weak interactions) regular amplitudes. However, we shall see in the next example that sometimes the suppression is absent, and then the diagrams with anomalous vertices become not only important, but also dominant, overshadowing all other contributions.

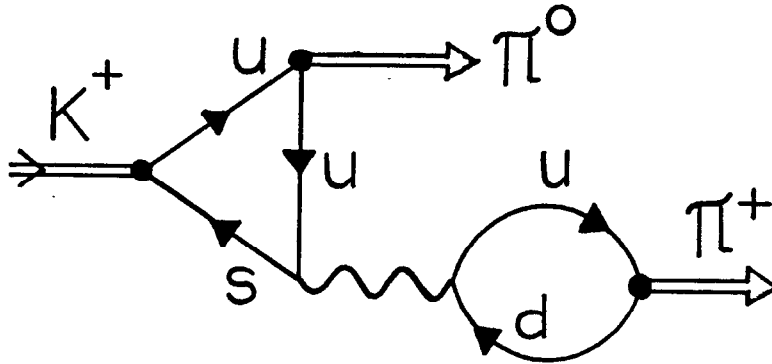


Fig. 10. A characteristic regular contribution to $K \rightarrow \pi\pi$.

Consider $K \rightarrow \pi\pi$ decays. We already know that diagrams with anomalous vertices should not contribute to $\Delta I = 3/2$ decays. Indeed, it is easy to demonstrate an exact cancellation of “anomalous” diagrams in $K^+ \rightarrow \pi^+ \pi^0$. A_{+0}^+ therefore receives a non-vanishing contribution A_{REG}^+ from the regular diagrams only. A characteristic diagram is presented in Fig. 10. The decay is Cabibbo suppressed, and of the first order in weak interactions. The amplitude can be written as^[6]

$$A_{+0}^+ = A_{\text{REG}}^+ \simeq \frac{G_{\text{FSC}}}{\sqrt{2}} M_K^2 f_\pi \cdot I \quad , \quad (15)$$

where $I \sim 1/2$ is a number whose exact value depends on the parameter n in (1). In Ref. 6 it was also shown that the regular contributions to the decays of K^S are of the same order, since the diagrams are very similar: $(A_{+-}^S)_{\text{REG}} \sim (A_{00}^S)_{\text{REG}} \sim A_{\text{REG}}^+$. This certainly can not account for the experimental results: we know that A^S amplitudes are much bigger. Could this time the diagrams with anomalous vertices make a difference? Consider diagrams for $K^S \rightarrow \pi^+ \pi^-$ sketched in Fig. 11 (A similar set can be constructed for $K^S \rightarrow \pi^0 \pi^0$). In $\pi_{\ell 2}$, the anomalous

contributions (Fig. 9) were negligible. On the contrary, by analysing Fig. 11, one finds no suppression! Although the encircled vertices are of the order G_F , they also change the flavor structure in such a way that no further weak interaction is needed to complete the decay. Consequently, the regular diagram (Fig. 10), and the diagrams with anomalous contributions (Fig. 11), are all of the same order in weak interactions.

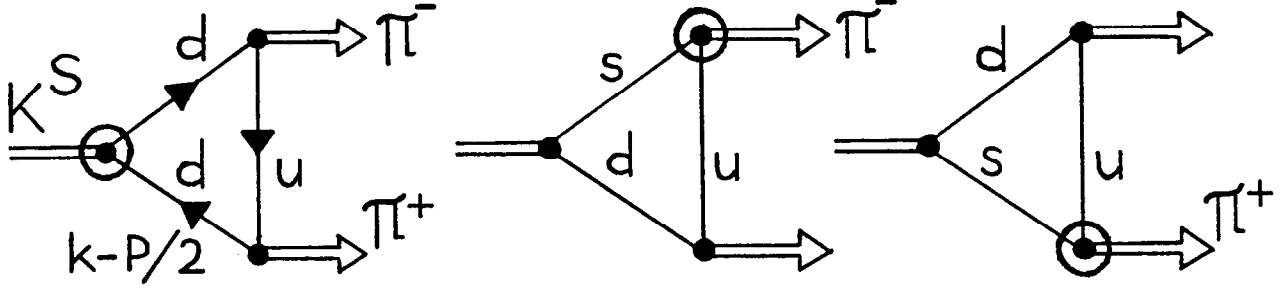


Fig. 11. Anomalous vertices in $K^S \rightarrow \pi^+ \pi^-$ decay.

According to the rules, the amplitude for the first diagram in Fig. 11 can be written after some rearrangement as

$$\begin{aligned} \tilde{A}(1) = & \frac{G_{FSC}}{\sqrt{2}} (\beta_K M_K^{2n-1}) (\beta_\pi M_\pi^{2n-3})^2 (-3) i^3 \int \frac{d^4 k}{(2\pi)^4} \\ & \frac{1}{\sqrt{2}} \left[\left(k + \frac{P}{2} \right)^2 - \left(k - \frac{P}{2} \right)^2 \right] \text{Tr} \left\{ \left(\not{k} + \frac{\not{P}}{2} - m_d \right) \frac{\not{P}(X + Y\gamma_5)}{B^{n+1}} \right. \\ & \left. \left(\not{k} - \frac{\not{P}}{2} - m_d \right) \frac{\not{S}\gamma_5}{C^n} \left(\not{k} + \frac{\not{S} - \not{R}}{2} - m_u \right) \frac{\not{R}\gamma_5}{D^n} \right\} . \end{aligned} \quad (16)$$

Here, the denominators are

$$B = k^2 - \alpha_K P^2, \quad C = (k - R/2)^2 - \alpha_\pi S^2, \quad D = (k + S/2)^2 - \alpha_\pi R^2, \quad (17)$$

and P, R, S are momenta of K^S, π^-, π^+ respectively. It is easy to see that $Y\gamma_5$ term from the anomalous vertex does not contribute. Indeed, traces of all terms

proportional to Y vanish. The analytic calculation with expressions similar to (16) is impractical, but after the evaluation of traces, one can calculate the remaining (convergent!) integrals numerically. Details of this calculation will be presented elsewhere. In our particular case, the amplitude (Eq. (16)) finally gets the form

$$\tilde{A}(1) = \frac{G_{\text{FSC}}}{\sqrt{2}} M_K^2 f_\pi X \cdot \tilde{I}(1) \quad . \quad (18)$$

(The sign “tilde” in this article will always be used to denote the anomalous contributions). X is the parameter from the anomalous vertex, and $\tilde{I}(1)$ a number which sharply depends on the model-parameter n . For $n = 5$, one, *e.g.*, finds $\tilde{I}(1) \approx 5$, and the ratio of the typical regular (Eq. (15)) and anomalous amplitudes becomes

$$(\tilde{A}(1)/A_{\text{REG}}^+)_{n=5} \sim (\tilde{I}(1)/I)_{n=5} X \sim 10 X \quad . \quad (19)$$

When the other two diagrams in Fig. 11 are evaluated, the complete anomalous amplitude \tilde{A}_{+-}^S for this decay approximately becomes $\tilde{A}_{+-}^S \sim 2\tilde{A}(1)$. Let A_{+-}^S denote the total (regular + anomalous) amplitude. The famous ratio A_{+-}^S/A^+ can now be expressed in terms of X . Indeed, from Eq. (19), one finds (for $n = 5$)

$$A_{+-}^S/A^+ \approx 2\tilde{A}(1)/A_{\text{REG}}^+ \approx 20 X \quad . \quad (20)$$

In the derivation of (20), I have neglected $(A_{+-}^S)_{\text{REG}}$, and have assumed $A_{+-}^S \approx \tilde{A}_{+-}^S$. It follows that if the model adopts the value for X close to 1, the successful parametrization of the $\Delta I = 1/2$ dominance can be achieved. For a different parameter n , a different value of X will do the job. Once the n is chosen and the constant X is fixed, the model gains a predictive power, which should be used in analyses of other processes. More on $K \rightarrow \pi\pi$, and some other K decays will be presented in the next section.

4. Detailed Study of Main Decay Modes of Kaons

In the previous section some important features of the model were briefly illustrated. This section is devoted to a detailed analysis of the main decay modes of K mesons. Parameters of both regular and anomalous vertices are fixed, and the theoretical results are compared to experiments. Finally, in the next section, the predictive power of the theory will be tested in an interesting rare decay.

We shall first consider processes in which the important contribution comes from diagrams with regular vertices only. The processes are listed in Table I. For completeness, not only K decays, but also $\pi_{\ell 2}$ and $\pi_{\ell 3}$ decays will be analyzed. Within the scheme, it is possible to describe all these leptonic and semileptonic decays by adjusting only two parameters, α_π and α_K . The results summarized in this section correspond to the choice $n = 5$, where n is the power in the denominators of vertex functions. Parameters α were determined in an analysis of $\pi^+ \rightarrow \mu^+ \nu$ and $K^+ \rightarrow \mu^+ \nu$ decays. The procedure is described in Ref. 6, and will not be repeated here. The correct decay rates are found with the values

$$\alpha_\pi^{(5)} = 2.387 \quad , \quad \alpha_K^{(5)} = 0.822 \quad . \quad (21)$$

The index in parentheses stands for $n = 5$. The above values correspond to $f_\pi = 130$ MeV, $f_K = 160$ MeV, $\beta_\pi = 1998.6$, and $\beta_K = 28.1$, see the expressions (7) and (8). Once the α 's are fixed, a straightforward procedure leads to the decay rates for other processes listed in Table I. A look at the Table reveals a general agreement between theoretical and experimental numbers. Only the results for $K_{\ell 3}$ decays deserve some further discussion. Let us consider one particular decay channel, $K^+ \rightarrow \pi^0 e^+ \nu$. (The arguments are similar for all the other $K_{\ell 3}$ decays). The diagrammatic calculation (see Fig. 12) gives the amplitude

$$A(K_{e3}^+) = -i \frac{G_F s}{\sqrt{2}} \frac{1}{\sqrt{2}} \{ (P+R)^\tau F_+^{K\pi}(Q^2) + (P-R)^\tau F_-^{K\pi}(Q^2) \} \bar{u}_\nu \gamma_\tau (1 - \gamma_5) v_e \quad . \quad (22)$$

P and R are momenta of the K^+ and π^0 , and $Q = P - R$ is the momentum

PROCESS	THEORY	EXPERIMENT
$\pi^+ \rightarrow \mu^+ \nu$	INPUT ^a	100%
$e^+ \nu$	1.3×10^{-4}	1.2×10^{-4}
$\pi^0 e^+ \nu$	1.0×10^{-8}	1.0×10^{-8}
$K^+ \rightarrow \mu^+ \nu$	INPUT ^b	0.64
$e^+ \nu$	1.6×10^{-5}	1.5×10^{-5}
$\pi^0 e^+ \nu$	0.035	0.048
$\pi^0 \mu^+ \nu$	0.023	0.032
$\Gamma(K_{e3}^+)/\Gamma(K_{\mu3}^+)$	0.66	0.66
$K^L \rightarrow \pi^- e^+ \nu$ [or $\pi^+ e^- \bar{\nu}$]	0.14	0.19
$\pi^- \mu^+ \nu$ [or $\pi^+ \mu^- \bar{\nu}$]	0.10	0.14
$K^- e^+ \nu$ [or $K^+ e^- \bar{\nu}$]	2.7×10^{-9}	n.a.
$\Gamma(K_{e3}^L)/\Gamma(K_{\mu3}^L)$	0.66	0.70
$K^S \rightarrow \pi^- e^+ \nu$ [or $\pi^+ e^- \bar{\nu}$]	2.5×10^{-4}	n.a.
$\pi^- \mu^+ \nu$ [or $\pi^+ \mu^- \bar{\nu}$]	1.6×10^{-4}	n.a.
$K^- e^+ \nu$ [or $K^+ e^- \bar{\nu}$]	4.7×10^{-12}	n.a.

Table I. Theoretical (with parameter $n = 5$) and experimental branching ratios for decays in which only diagrams with regular vertices contribute. The first two significant digits are displayed in the results. Comments: (a) Input for α_π ; (b) Input for α_K .

transferred to leptons. For $n = 5$, the form factors are defined as^[6]

$$F_{\pm}^{K\pi}(Q^2) = (\alpha_{\pi}\alpha_K)^4 (M_{\pi}M_K)^7 \int_0^1 dx \frac{630x^4(1-x)^4}{[(1-x)M_{\pi}^2 \pm xM_K^2] [(1-x)\alpha_{\pi}M_{\pi}^2 + x\alpha_KM_K^2 - \frac{1}{4}x(1-x)Q^2]^8} . \quad (23)$$

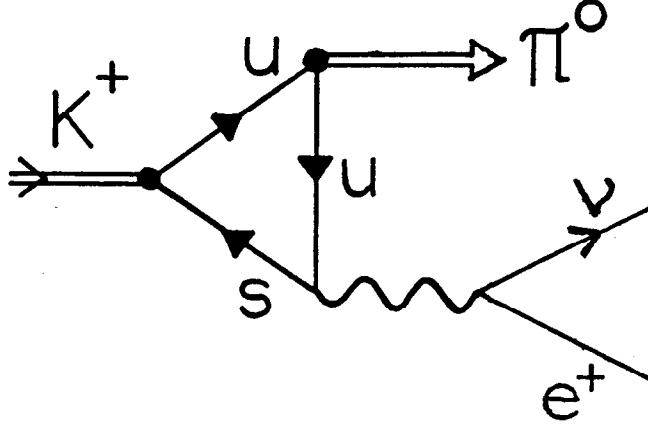


Fig. 12. Decay $K^+ \rightarrow \pi^0 e^+ \nu$.

Since the expression (22) has the standard form^[12-14], the disagreement between the theory and experiments must have been caused by the numerical values of the functions given in (23), or more precisely — by the magnitudes of $F_{+}^{K\pi}$ and $F_{-}^{K\pi}$ at $Q^2 \sim 0$. In the case of an ideal SU(3) symmetry, these values would have been equal to 1 and 0 respectively. In the real world SU(3) is broken, but the symmetry breaking is believed to produce only the second order effects, making *e.g.*, the form factor $F_{+}^{K\pi}(0)$ just slightly smaller than 1. The SU(3) breaking in the model described in Sect. 2, is — on the other hand — directly related to the masses of π and K , and the form factors are more strongly affected. With the parameters (21), one finds $F_{+}^{K\pi}(0) = 0.763$, and $F_{-}^{K\pi}(0) = -0.472$. As a consequence, the amplitude and the branching ratio become smaller than expected. One could probably push all the K_{l3} branching ratios higher by playing with parameters and by changing the form of wave functions. However, such a procedure

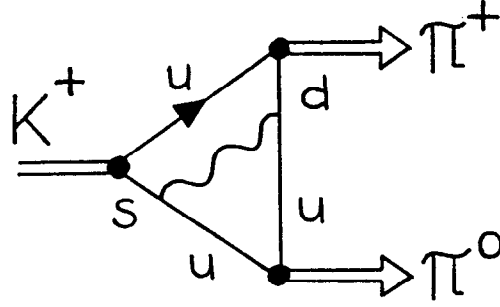


Fig. 13. Color suppressed regular diagram for $K^+ \rightarrow \pi^+\pi^0$ decay. The amplitude comes out to be $1/3$ ($= 1/N$) of the value resulting from the diagram in Fig. 10. Here, N is the number of colors.

would not significantly increase our understanding, and therefore no fine tuning was attempted in this work. After all, though slightly too small, the amplitudes for $K_{\ell 3}$ decays are almost at the target.

It is easy to see that in all the decays considered in Table I, the anomalous contributions are many orders of magnitude smaller than the regular one, and could therefore be safely neglected. A different situation occurs in $K^+ \rightarrow \pi^+\pi^0$ decay. Individual diagrams with anomalous vertices in this decay are *not* suppressed. However, when all the diagrams are summed, the total anomalous contribution adds exactly to zero. As explained earlier, the cancellation is related to the isospin structure of the anomalous vertices. Consequently, even in this process, only the diagrams with regular vertices determine the amplitude. The relevant diagrams are presented in Figs. 10 and 13. With form factors $F_{\pm}(Q^2)$ as defined in (23), the total amplitude for $K^+ \rightarrow \pi^+\pi^0$ decay can be written as

$$A_{+0}^+ = \left(1 + \frac{1}{3}\right) \frac{G_F^{\text{sc}}}{\sqrt{2}} M_K^2 f_{\pi} \frac{1}{\sqrt{2}} \left\{ \left(1 - \frac{M_{\pi}^2}{M_K^2}\right) F_+^{K\pi}(M_{\pi}^2) + \frac{M_{\pi}^2}{M_K^2} F_-^{K\pi}(M_{\pi}^2) \right\}. \quad (24)$$

The result (24) is very similar to the old “vacuum saturation” result^[15]. Our model, however, not only gives the form, but also determines the values of form factors F_{\pm} . The first summand in the factor $(1 + 1/3)$ comes from the diagram in Fig.

10. The second one, namely $1/3 \equiv [\text{color}]^{-1}$, originates from the diagram in Fig. 13, indicating that this diagram is “color suppressed”. Numerically, the amplitude (for $n = 5$ model) becomes $A_{+0}^+ = 39$ eV. The measured value, however, is about two times smaller. Obviously, in hadronic decays our simple model does not work as good as in the semileptonic decays. It produces the right order of magnitude for the A_{+0}^+ amplitude, but can not do much better than that. A minor adjustment of wave functions, mentioned in the discussion of the semileptonic amplitudes, would not help here. It is more likely that some important feature is not completely covered by the presented simple version of the model. *E.g.*, it is possible that in the scheme in which explicit gluons are forbidden, the color suppressed diagrams get overestimated. Indeed, it is easy to see that the agreement with experiments becomes better if those diagrams (see Fig. 13) are neglected. Another possibility is that the relative sign between diagrams in Figs. 10 and 13 is different. With the change of the sign, the factor $1 + 1/3 = 4/3$ would become $1 - 1/3 = 2/3$, and the amplitude would be reduced just by two, as required. However, the relative sign between diagrams is directly related to the adopted rule “minus sign for each closed fermion loop”. The sign would change if we disobey the rule, but presently I see no justification for such a step other than to obtain an agreement with experiments. Another interesting proposal was put forward by Scadron^[16], several years ago. He suggested a replacement of the factor $G_F/\sqrt{2}$ by $G_F/2\sqrt{2}$ in all hadronic decays, due to a symmetrization $J^\dagger J \rightarrow \frac{1}{2}(J^\dagger J + J J^\dagger)$, and a noncommutativity of the hadronic currents. The receipt was successfully applied in a study of decays of charm particles^[16]. Such a factor $1/2$ would clearly also help in $K^+ \rightarrow \pi^+\pi^0$ decay. It would reduce expression (24) just to the right value. Finally, it might happen that the difference is caused by the SD QCD corrections, which were neglected in the first approximation. This possibility was thoroughly discussed long ago in the landmark papers by Gaillard and Lee^[2], and Altarelli and Maiani^[3]. I do not expect SD QCD to account for the huge factor 20 in the $\Delta I = 1/2$ rule, but might accept that it changes some results for a factor of 2. Obviously, there are many possible directions for an improvement of the scheme, and one should find out which

one fits most naturally into the model. Admittedly, the factor 2 disagreement in the amplitude is a serious problem^[17], but I hope that this is a “curable disease”. Therefore, I will continue the analysis of the remaining two-body hadronic decay modes, keeping in mind, however, that due to theoretical uncertainties the model could be trusted only to a certain degree, *e.g.*, up to a factor of 2 or 3.

Decay	Model A	Model B	Experiment
$K^+ \rightarrow \pi^+\pi^0$	0	0	18 eV
$K^S \rightarrow \pi^+\pi^-$	$(285 X_{(5)}^A) \text{ eV}$	$(-55 X_{(5)}^B) \text{ eV}$	389 eV
$K^S \rightarrow \pi^0\pi^0$			372 eV
$K^L \rightarrow \pi^+\pi^-$	0	0	0.9 eV
$K^L \rightarrow \pi^0\pi^0$			0.8 eV

Table II. Amplitudes for $K \rightarrow \pi\pi$ decays. The anomalous contributions, calculated in models A and B (with $n = 5$), are compared to experimental results. The latter were obtained from the measured decay rates^[18], by using $|A_{\text{EXP}}| = (8\pi M_K^2 \Gamma / |\vec{p}|)^{1/2}$. The statistical factor $\sqrt{2}$ is included in $(A_{00}^{S,L})_{\text{EXP}}$.

The full advantage of the anomalous vertices can be seen in the study of decays of the neutral kaons. Though the regular vertices also contribute to K^L and K^S decays, they can not account for more than 15 % of the total A_{00}^S or A_{+-}^S .

amplitudes. Indeed, it was shown in Ref. 6, that

$$\begin{aligned} (A_{00}^S)_{\text{REG}} &= +\frac{1}{2}A_{+0}^+ & , & & (A_{+-}^S)_{\text{REG}} &= -\frac{3}{2}A_{+0}^+ & , & & (25) \\ (A_{00}^L)_{\text{REG}} &= 0 & , & & (A_{+-}^L)_{\text{REG}} &= 0 & . \end{aligned}$$

(Note that the second line in (25) reflects the absence of CP violation in the four-flavor model). Numerically, the $(A^S)_{\text{REG}}$ amplitudes are not bigger than 50 eV, while the experimental numbers are on the order of 400 eV. From now on, I will therefore totally neglect the regular diagrams in the analysis of the $K^S \rightarrow \pi\pi$ decays, and rely only on diagrams with anomalous vertices. Within the scheme, the first to consider are the diagrams in which only one of the regular vertices is replaced by a vertex with an anomalous flavor structure. Such diagrams for $K^S \rightarrow \pi^+\pi^-$ decay are depicted in Fig. 11, and one of the amplitudes, $\tilde{A}(1)$, is displayed in Eq. (16). The remaining two amplitudes are

$$\begin{aligned} \tilde{A}(2) + \tilde{A}(3) &= \frac{G_{\text{FSC}}}{\sqrt{2}} (\beta_K M_K^{2n-3}) (\beta_\pi M_\pi^{2n-2})^2 (-3) i^3 \int \frac{d^4 k}{(2\pi)^4} \\ &\frac{1}{\sqrt{2}} \left[\left(k + \frac{P}{2} \right)^2 \text{Tr} \left\{ \left(\not{k} + \frac{\not{P}}{2} - m_s \right) \frac{\not{P}\gamma_5}{B^n} \left(\not{k} - \frac{\not{P}}{2} - m_d \right) \frac{\not{S}\gamma_5}{C^n} \right. \right. \\ &\left. \left(\not{k} + \frac{\not{S} - \not{R}}{2} - m_u \right) \frac{\not{R}(X + Y\gamma_5)}{D^{n+1}} \right\} - \left(k - \frac{P}{2} \right)^2 \text{Tr} \left\{ \left(\not{k} + \frac{\not{P}}{2} - m_d \right) \right. \\ &\left. \left. \frac{\not{P}\gamma_5}{B^n} \left(\not{k} - \frac{\not{P}}{2} - m_s \right) \frac{\not{S}(X + Y\gamma_5)}{C^{n+1}} \left(\not{k} + \frac{\not{S} - \not{R}}{2} - m_u \right) \frac{\not{R}\gamma_5}{D^n} \right\} \right] . \end{aligned} \quad (26)$$

The denominators B, C , and D were defined in Eq. (17). When contributions of all three diagrams are summed, the total *anomalous* amplitude can be written as

$$\tilde{A}_{+-}^S = \frac{G_{\text{FSC}}}{\sqrt{2}} M_K^2 f_\pi X \cdot \tilde{I} \quad . \quad (27)$$

Here, \tilde{I} denotes a sum of loop integrals which must be calculated numerically. In the Model A, with $n=5$, one finds $\tilde{I} \rightarrow \tilde{I}_{(5)}^A = 5.00$. (For the Model B results, see

Appendix B). X in (27) is the unknown parameter, sitting in the anomalous vertex, see Eq. (4). One also easily finds that $\tilde{A}_{00}^S = \tilde{A}_{+-}^S$. The anomalous amplitudes in terms of the parameters X are given in Table II, for both Model A and Model B. If the anomalous vertices are responsible for the $\Delta I = 1/2$ dominance, the free parameters must assume the values,

$$X_{(5)}^A \simeq 1.3 \quad (\text{Model A}) \quad , \quad X_{(5)}^B \simeq -6.8 \quad (\text{Model B}) \quad . \quad (28)$$

With these values, two $K^S \rightarrow \pi\pi$ amplitudes get the magnitude of about 376 eV. The remaining fine splitting between $(A_{00}^S)_{\text{EXP}}$ and $(A_{+-}^S)_{\text{EXP}}$ could be achieved if the small regular contributions (25) are added to the anomalous amplitudes with a certain phase angle. It is also important to note that in $K^S \rightarrow \pi\pi$ decays only the parameter X can be determined, but nothing can be said about the other parameter characterizing anomalous vertices, namely Y (see Eq. (4)). As a working hypothesis we can assume that this parameter has a value not too different from X , and set $Y \approx X$. However, this is only a hypothesis, which still has to be confirmed (or rejected) in analyses of other decay channels.

What have we seen so far is that the diagrammatic calculation in the long-distance scheme can accommodate to a good degree of accuracy all the major decay modes of K (and π), provided the parameter X has the proper value. It remains to examine the predictive power of the model. That will be done in the next section, in an analysis of one interesting, though not yet observed, decay mode of K^+ .

5. K Decays and Fifth Force

Once we are convinced that some model successfully describes the basic K decays, we usually apply the model in a subsequent study of rare and/or unobserved kaon decays. This has repeatedly been done in the past, and will also be carried out in this work. Only such a procedure truly tests the predictive power of a scheme. Indeed, while a theoretical study of *e.g.*, $K \rightarrow \pi\pi$ decays is always in one or the other way affected by the well measured experimental numbers, the real nature of a model is revealed only when one is not in temptation of reproducing some of the firmly established data.

The decay channel which will be analysed in this section is $K^+ \rightarrow \pi^+\gamma_Y$. Here, γ_Y is the “hyperphoton” — an ultra-light vector particle (with the mass possibly smaller than 10^{-8} eV) associated with the so-called fifth force^[19]. This force might be responsible for effects observed in recent experiments measuring deviations from the ordinary gravity^[20–25]. Note that the deviations in some of these experiments might also be a sign of a short range quantum fluctuation in gravitational theory, and thus possibly unrelated to the fifth force. It would be much easier to distinguish between the two competing hypotheses if a clear effect is observed also in K decays. This is the main reason for renewed interest in $K^+ \rightarrow \pi^+\gamma_Y$. Indeed, a better experimental limit and a reliable theoretical description of this decay, could lead us to a firm confirmation of the fifth force, and give an important piece of information on its character and strength. Several excellent articles^[26–29] about the new force were published recently, and the reader is referred to these reviews for further details. Presently, the experimental limit^[30] on the branching ratio for $K^+ \rightarrow \pi^+\gamma_Y$ decay is $B < 4.6 \times 10^{-8}$. A new experiment^[31] is expected to push this limit to the range 10^{-10} in the near future. The decay has also been studied by four groups of theorists^[32–35]. An essential step in all the theoretical analyses was to relate matrix elements of $K \rightarrow \pi\gamma_Y$ to those of $K \rightarrow \pi\pi$ decays, and each group devised different methods to achieve that goal. Surprisingly, the quoted results for the branching ratio are spread over two orders of magnitude (see Table III). It

will be interesting to see how our long-distances oriented model, with the direct evaluation of amplitudes, compares to the other analyses.

The coupling of the hyperphoton to a quark can be described by the vertex $i f C_q \gamma^\tau$, where f denotes the general strength of the fifth force, and C_q is the hypercharge of the interacting quark. For example, $C_u = C_d = 1/3$, $C_s = -2/3$, $C_c = 4/3$, etc. In the nonrelativistic limit, the above form of the vertex corresponds to the Yukawa potential $V = (f^2/4\pi) \exp(-br)/r$. Note that Fischbach's group^[27-29,33] uses a different Yukawa coupling, and their constant f^2 is 4π times smaller than the one used here. (This fact is important in the numerical comparison of various results, and has been taken into account in the Table III).

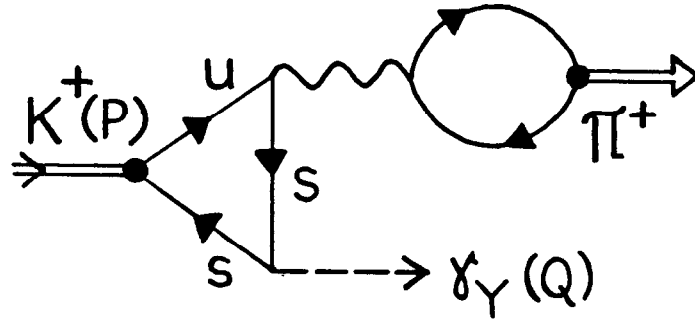


Fig. 14. One of the regular diagrams for $K^+ \rightarrow \pi^+ \gamma_Y$ decay. Hyperphoton can be emitted by any of the quarks. Thus, three additional diagrams should also be considered.

Two classes of diagrams have to be considered in an analysis of $K^+ \rightarrow \pi^+ \gamma_Y$ decay. In the first class, the diagrams are constructed without use of the anomalous vertices. A typical diagram is presented in Fig. 14. When three similar diagrams are added, and the amplitude calculated with α 's and β 's as determined in (21), one finds

$$A_{\text{REG}}^\tau = -i \frac{G_F^{sc}}{\sqrt{2}} f f_\pi f_K [0.042] P^\tau + \dots \quad (29)$$

P^τ is the momentum of the kaon. The dots denote the part of the amplitude

proportional to the hyperphoton momentum Q^τ . (This latter piece does not affect the decay rate). Had (29) been the only contribution, the branching ratio would have been of the order $B \sim 2 \times 10^{13} (f/m_Y)^2 \text{ eV}^2$, which is much smaller than B obtained in the other analyses^[32-35], and beyond the present experimental limit. However, we know that the second class of diagrams, those with anomalous vertices, should also be considered. They are presented in Fig. 15.

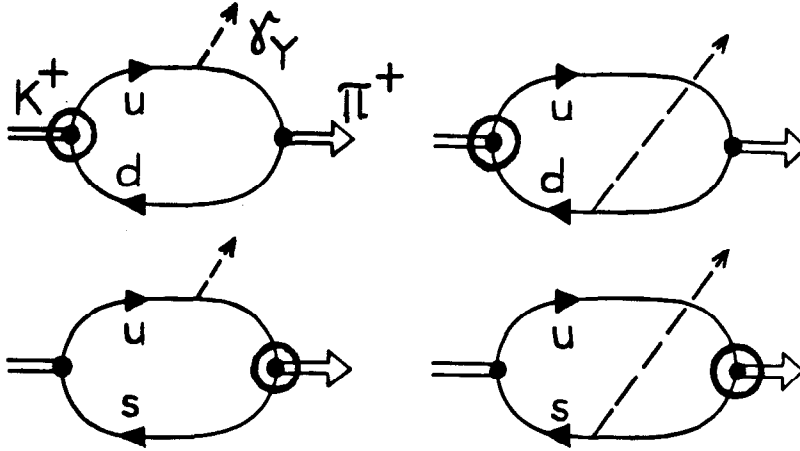


Fig. 15. The four diagrams with anomalous vertices.

In the Model A, after some rearrangement, the sum of the corresponding amplitudes can be written as

$$A_{\text{ANOM}}^\tau = \frac{G_{\text{FSC}}}{\sqrt{2}} (\beta_K M_K^{2n-3}) (\beta_\pi M_\pi^{2n-3}) f Y (-3) \int \frac{d^4 k}{(2\pi)^4} \quad (30)$$

$$\left[M_K^2 \frac{C_u J^\tau(1) - C_d J^\tau(2)}{V^{n+1} U^n} + M_\pi^2 \frac{C_u J^\tau(3) - C_s J^\tau(4)}{V^n U^{n+1}} \right] ,$$

where

$$V = k^2 - \alpha_K M_K^2 \quad , \quad U = (k + Q/2)^2 - \alpha_\pi M_\pi^2 \quad , \quad (31)$$

and

$$\begin{aligned}
J^\tau(1) &= \left(k + \frac{P}{2}\right)^2 \text{Tr} \left\{ \gamma^\tau \not{P} \left(k + \frac{P}{2}\right) \not{R} \right\} = J^\tau(3) \quad , \\
J^\tau(2) &= \left(k - \frac{P}{2}\right)^2 \text{Tr} \left\{ \gamma^\tau \not{R} \left(k + \frac{P}{2}\right) \not{P} \right\} \quad , \\
J^\tau(4) &= \left(k - \frac{P}{2} + Q\right)^2 \text{Tr} \left\{ \gamma^\tau \not{R} \left(k + \frac{P}{2}\right) \not{P} \right\} \quad .
\end{aligned} \tag{32}$$

When all the traces are calculated, and the loop integrals evaluated, the relevant part of the “anomalous” amplitude in Model A, with $n = 5$, becomes

$$A_{\text{ANOM}}^\tau = -i \frac{G_{\text{F sc}}}{\sqrt{2}} f f_\pi f_K [4.7116 Y_{(5)}^A] P^\tau + \dots \quad . \tag{33}$$

In a similar way A_{ANOM}^τ can be calculated in the Model B (for the result see Appendix B). It is important to note that the amplitude (33) is proportional to the parameter Y from the anomalous vertex (4), and not to X which played a role in the $K \rightarrow \pi\pi$ decays. This is the place where the assumption $X \approx Y$ (discussed after Eq. (28)) enters. If one uses $Y_{(5)}^A = 1.3$ (compare to Eq. (28)), it becomes clear that the anomalous amplitude (33) completely dominates over the regular one, Eq. (29). Consequently, $K^+ \rightarrow \pi^+ \gamma_Y$ is another process in which regular diagrams could be totally neglected: diagrams with $s \rightarrow d$ transitions contain all the important physics! (A similar conclusion follows also in Model B). When the absolute square of the amplitude is multiplied by the appropriate phase-space factor, and divided by the total width, one finds the branching ratio B . For Model A, this becomes

$$B = 26.7 [Y_{(5)}^A]^2 \frac{f^2}{m_Y^2} \times 10^{16} \text{ eV}^2 \quad . \tag{34}$$

Here, m_Y is the mass of the hyperphoton. In Table III, parameters Y^A (and Y^B) are replaced by their numerical values, and the branching ratios are expressed in terms of the unknown quantity $(f/m_Y)^2$.

Ref.	B (in 10^{16} eV^2)	COMMENT
Aronson <i>et.al.</i> ^[33]	0.5 (f^2/m_Y^2)	(a)
Suzuki ^[32]	4.4 (f^2/m_Y^2)	(b)
	35.4 (f^2/m_Y^2)	(c)
Bouchiat <i>et.al.</i> ^[34]	30.0 (f^2/m_Y^2)	(d)
Lusignoli <i>et.al.</i> ^[35]	31.0 (f^2/m_Y^2)	
this work	45.0 (f^2/m_Y^2)	(e)
	2.5 (f^2/m_Y^2)	(f)

Table III. Various theoretical predictions for the branching ratio $B = \Gamma(K^+ \rightarrow \pi^+\gamma_Y) / \Gamma(K^+)_{\text{ALL}}$. All the results are given in terms of f^2 normalized according to the convention described in the text. Comments: (a) The common four-momentum in two-body matrix elements is taken to be the pion momentum; (b) With $r^2 = 1.5$ (r^2 is an enhancement factor due to a presence of the short-distance gluons); (c) With $r^2 = 12$; (d) Corresponds to $x = 0.29$ choice. (x is a correction factor required because of an extrapolation to the zero-momentum pion); (e) Model A, assuming $Y_{(5)}^A = X_{(5)}^A = 1.3$; (f) Model B, assuming $Y_{(5)}^B = X_{(5)}^B = -6.8$.

From the theoretical viewpoint, it is significant that the Model A and Model B results are so different, although both models gave the identical description of $K \rightarrow \pi\pi$. Clearly, the choice of wave functions plays the major role in a study of rare decays, and this is true not only for our diagrammatic approach, but also – as seen from Table III – for all previous analyses. The big spread of the results basically reflects our inability to deal with long distance physics. An optimistic view, that if we can correctly describe the main K decay modes it automatically means we can trust the method in rare decays, is not at all supported by the above study^[36]. Fortunately, in our example the physical consequences are unaffected. Even the lowest branching ratio in Table III seems to be excluded by experiments.

Indeed, an upper limit on the strength of the fifth force can be deduced from the Table, and one finds

$$\frac{f^2}{m_Y^2} \leq 9.2 \times 10^{-24} \text{ eV}^{-2} = 60 G_\infty m_H^2 [\text{meter}]^2, \quad (35)$$

where G_∞ is the gravitational constant, and m_H is the hydrogen mass. The upper bound (35) is not in agreement with findings from geophysical and other experiments. Therefore, it was suggested^[37] that the fifth force might be coupled not exclusively to the hypercharge, but rather to a combination of hypercharge, strangeness and isospin. Then a window for a superlight, vector carrier of the fifth force is still open.

As a final remark, let me repeat that results in the Models A and B were obtained with the assumption that $Y \approx X$. With this assumption, the results more or less fit into the broad region charted by the other studies of the process. However, if by some reason it comes out that $Y \ll X$, the picture changes completely. In that case, the branching ratio for $K \rightarrow \pi\gamma\gamma$ process becomes very small, and possibly even dominated by *regular* diagrams. As a consequence, even the pure hypercharge coupling of the fifth force could be saved. This possibility will be thoroughly discussed in another work.

6. Concluding Remarks

Almost every physical problem can be approached from various starting points. This is also true for problems encountered in K decays. In recent years we have seen many attempts to explain $\Delta I = 1/2$ rule, CP-violation, and other phenomena related to kaons, by assuming the short-distance dominance and usefulness of the operator expansion. Even in analyses on lattices, sets of SD operators played a significant role,^[38-40]. On the other hand, it was somewhat frustrating to see that alternative models, built on different concepts, did not meet wider attention. In this work I am introducing a model that perhaps could successfully compete with the simplicity of the standard SD approaches, although it is based on directly opposite set of starting assumptions. Short distance QCD corrections are completely neglected, and all other QCD corrections are absorbed in some highly nonlocal vertex functions. The trade marks characterizing this new scheme are probability distributions sitting in quarks-meson vertices, and the use of diagrams in a direct calculation of full amplitudes.

The probability distributions are related to wave functions of mesons, and – as explained earlier – they appear in two different varieties: the regular and the anomalous one. The regular distributions give probabilities of finding the standard quark contents within a given meson. An anomalous distribution takes into account the possibility that one of the quarks within a meson undergoes a change of flavor due to the weak interactions. Our study of vertices and diagrams shows that two typical situations might occur. Very often diagrams with anomalous vertices are either completely forbidden or of the second order in weak interactions, and consequently highly suppressed. In such situations the amplitudes of the corresponding processes are determined by regular diagrams only. There is also a second type of processes, in which the suppression does not happen, and both regular and anomalous contributions are possible. We can “postulate” that in the latter situation the anomalous contributions absolutely dominate over the regular one. The best support for this “postulate” comes from $K \rightarrow \pi\pi$ decays: $K^+ \rightarrow$

$\pi^+\pi^0$ is in the first category (anomalous vertices are forbidden), while the similar decays of K^S and K^L are in the second. Clearly, any parametrization of vertices which makes anomalous amplitudes much bigger than a similar regular one, leads immediately to the $\Delta I = 1/2$ dominance and “explains” large A^S and surprisingly big CP-violating A^L amplitudes. Of course, the “postulate” and the “explanation” mentioned above were dictated by known experimental facts. However, once the measured values are used to fix a few parameters of the model, a certain degree of the predictive power is achieved, and the model becomes a useful tool in analyses of other processes.

The assumption that all important physics is hidden in regular and anomalous wave functions clearly reveals the long-distance character of the scheme. Therefore, the parallel use of diagrams might at first look strange. Indeed, we are accustomed to see diagrams in perturbative calculations, but not in analyses of long-distance, and thus nonperturbative phenomena. However, a closer inspection shows that the diagrams primarily have a book-keeping role. Basically, we are still dealing with various probabilities (*e.g.*, the probability of finding a quark within the meson, likelihood of propagation of that quark, *etc.*), and diagrams help to account correctly for these probabilities and their summation. Another good thing about the diagrams is that they enable a better qualitative understanding of decay processes, in terms of clear physical pictures. The processes are not shattered into pieces which are then treated separately. On the contrary, a full diagram reminds us that the related process should be considered as an irreducible unit.

In addition to some of the above mentioned desirable properties, the scheme also has its dark sides. There are two kinds of problems which yet have to be attacked and – hopefully – overcome. The first category was already discussed throughout the text, and is closely related to phenomenology. Not only that we need better probability distributions (*i.e.*, “wave functions”), but also a theory which will shed some light on the form and parameters of the distributions. (Presently, the form is imposed by the requirement of simplicity, and the parameters determined from experiments). The factor two debacle in $K^+ \rightarrow \pi^+\pi^0$ decay

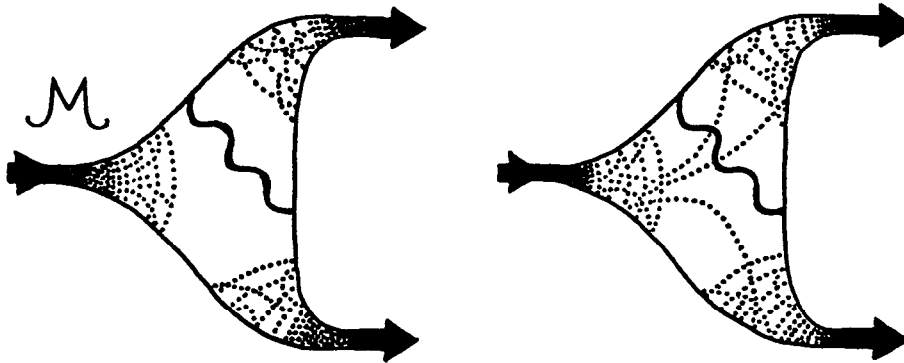


Fig. 16. Two-body hadronic weak decay of a meson. Dots indicate gluonic corrections.

will most likely dictate introduction of one additional “rule” to our list.

There is also a second class of problems, inherent to the scheme itself. Consider, *e.g.*, Fig. 16. The left diagram is properly treated by the model. The denoted QCD corrections are already included in the effective vertices, and with appropriately chosen probability distributions there should be no problems with that type of diagrams. A different situation is presented in the right diagram. Here, some gluons are allowed to be exchanged between different effective vertices. These QCD corrections are certainly not accounted for in the scheme. How important are they? In some of these diagrams, the momentum flow reveals a dominance of momenta of the order M_W , and thus they represent the SD QCD corrections. The latter – according to the scheme – are not so important and could be ignored in the first approximation. In the remaining diagrams in which gluons connect effective vertices, the dominant loop momenta are unfortunately not related to M_W . Consequently, it becomes very difficult to say anything about the importance of diagrams from that subgroup. The scheme automatically ignores them, but I do not know how seriously this affects the results.

Closely related is a problem caused by gauge invariance of the underlying theory. It is easy to see that the required invariance forces us to introduce higher

Fock states in all wave functions of mesons. This is illustrated in Fig. 17, and more thoroughly discussed in Ref. 7. For each nonlocal vertex $\mathcal{M}(q\bar{q}')$, there should exist related vertices with one, two, *etc.*, gauge particles (photons, gluons, W -bosons) attached to the prime vertex. Whenever we opt for the lowest Fock states only (and this, as a rule, has been done in most of the existing analyses), we jeopardize the gauge invariance. The *radiative* decays were not considered in this work just for that reason. In principle however, the model could be expanded in such a way that it also includes *e.g.* $\mathcal{M}(q\bar{q}')\gamma$ vertices. This expansion is a must if radiative K decays are to be considered in the model. (In a similar way, W can be introduced into vertices. However, there are some indications^[9], that this will not affect results described in Sections 4 - 6).

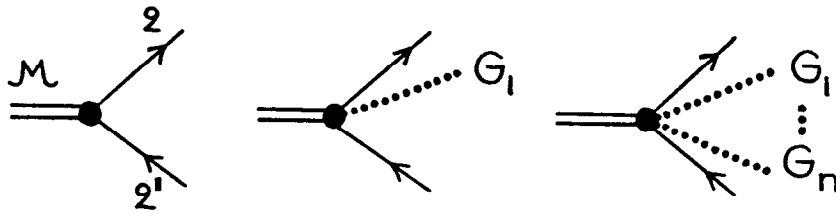


Fig. 17. The gauge invariance dictates appearance of higher Fock states in effective (both regular and anomalous) vertices. G denotes a gauge particle, *e.g.*, a gluon or a photon.

In conclusion, the first step has been made in a development of a new scheme for the study of K decays. Main features, the dominance of LD corrections, evaluation of the complete amplitudes, and importance of $s \rightarrow d$ transitions, are unified in a simple, effective model. A need (and also a possibility) for significant improvements exists, but even in the present form, the model enables a look at some interesting aspects of K decays not previously studied. Further improvements of the scheme, and a better general understanding of QCD and confinement, might eventually bring us closer to the final solution of one of the major problems in hadronic weak interactions.

Acknowledgments: It would have been impossible to complete this work without support, encouragements, and – yes – criticism of many friends, particularly J. Eeg, E. Fischbach, B. Guberina, I. Picek, M. Scadron and D. Tadić. I also want to thank R. Blankenbecler for the kind hospitality in the SLAC Theory Group.

The situation changed in early 70's. Three quarks became a reality, and the fourth was anticipated^[41]. In 1971, the Glashow–Salam–Weinberg model was shown by t'Hooft to be renormalizable, and two years later, thanks to the property of asymptotic freedom, the QCD became the main candidate for the theory of strong interquark forces. At that time, $s \rightarrow d$ transitions reentered analyses of K decays, now truly in the quark environment: Gaillard and Lee^[2] considered various two-body $[\bar{d}s]$ operators, but eventually decided against their use in an effective, strangeness changing Hamiltonian. They discovered that some of the operators were suppressed by the GIM mechanism^[41], while the others could have been transformed away by redefinitions of fields. It should be noted that instead of diagrams, the operators now became the main subject of interest, and there were several reasons for this change. First, it was believed that interactions of quarks bound in hadrons were – at short distances – properly described by scattering of (almost) free quarks. The scattering amplitude corrected by QCD, could in turn be described by field operators. Thus, an “effective Hamiltonian” consisting of quark fields, could have carried at least some information relevant for a hadronic physical process. The Hamiltonian formalism had been known and loved in analyses of *leptonic* weak interactions for many years, and Hamiltonians built up of *hadronic currents* were also widely used in pre-quarks days^[12]. It was therefore natural to use a knowledge gained with old Hamiltonians to relate matrix elements of the new multiquark operators to physical decay amplitudes. There was yet another advantage of dealing with operators: a systematic study of certain QCD corrections to *diagrams* was possible by studying the renormalization of corresponding *operators*. Indeed, the renormalization group equation, when applied to Green functions with operator insertions, reveals coefficients of the leading $(g^2 \ln \mu^2)^n$ terms. Here, $\mu^2 < 0$ is a “renormalization point”, and g is the QCD coupling constant. By dimensional reasons, the same coefficients appear with the leading $(g^2 \ln M^2)^n$ terms in related diagrams, where M is a large scale in the process (often a mass of the weak boson). It should be remembered that although diagrams of a physical process and quark operators in a Hamiltonian are related, in hadronic physics these two concepts still

ought to be distinguished. The fact that quarks are tightly bound in hadrons is not always properly reflected in the effective Hamiltonians, and in some cases this might be a source of confusion. (On the contrary, in leptonic processes, where asymptotic states are free spinors, diagrams and leptonic operators may be used interchangeably).

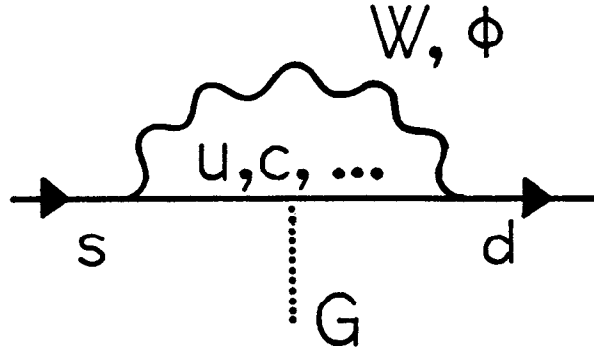


Fig. A2. A gluon is emitted from the loop, and the GIM suppression disappears.

Following the Gaillard and Lee conclusions^[2], physicists for a while ignored the $s \rightarrow d$ transitions in studies of K decays. However, in 1977, these transitions got a big push indirectly, in a work by Shifman, Vainshtein and Zakharov^[42]. These authors realized that diagram in Fig. A2 was not suppressed by the GIM mechanism, thus being of the order G_F rather than G_F/M_W^2 . To find the “short distance” contribution of series of diagrams in Fig. A3, Shifman *et al.*^[42] constructed the (“penguin”) operator, $[\bar{d}\gamma^\mu(1 - \gamma_5)t^a s]D_{ab}^\nu G_{\nu\mu}^b$, and analysed it via the renormalization group. (D_{ab}^ν is a covariant derivative acting on the gluon energy momentum tensor). They were able to collect all QCD corrections of the form $(g^2 \ln m_c^2)^n$. Though of the right order, the coefficient of the penguin operator still came out to be very small. The hope was that this might be compensated by an enhancement in calculation of matrix elements, expected because of an unusual chiral structure of the operator. Despite some controversy, the penguin terms became a standard

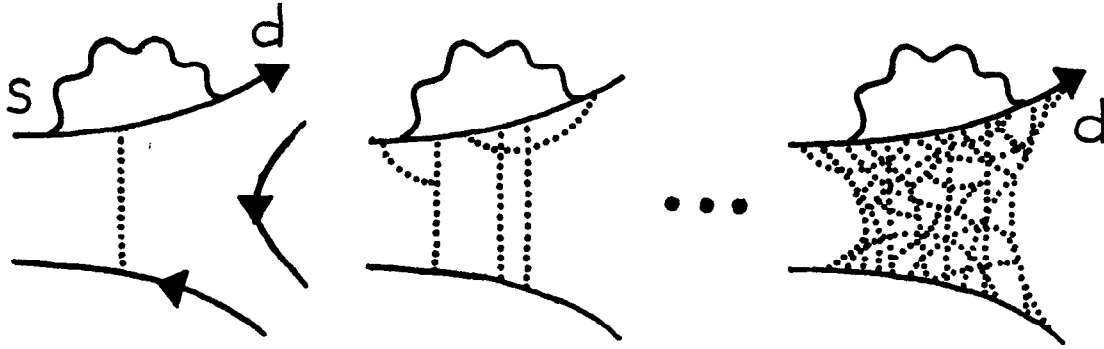


Fig. A3. A class of QCD corrections related to $s \rightarrow d$ transitions. The third quark line, which acted as a “spectator” in Shifman *et al.* analysis, is denoted only in the first diagram.

part of the effective Hamiltonian approach, and caused a renewed interest in the $s \rightarrow d$ transitions.

Not everybody was thrilled by a calculation of amplitudes in terms of two-body matrix elements of operators. A “diagrammatic” approach, with a direct calculation of complete amplitudes, was attempted by Pascual and Tarrach^[9]. They introduced local quark–meson vertices, and absorbed strong interactions effects into phenomenological weak decay constants, f_K, f_π , and in constituent quark masses. By neglecting external momenta, they were able to calculate physical amplitudes in terms of simple momentum space integrals. A big enhancement for diagrams with $s \rightarrow d$ transitions (Fig. A4) was reported. The strongest criticism of their work comes from the fact that authors did not include all “self-energy” diagrams into analysis. It was argued (see *e.g.* the work by Chia^[43]) that missing diagrams, with an unphysical Higgs particle, would have cancelled the dominant G_F contribution found in Ref. 9, making diagrams in Fig. A4 too small to be important. We shall see later that such a criticism, though perfectly valid in a general analysis of the renormalization of $s - d$ self-energy, might not be as devastating in the special situation described by Pascual and Tarrach^[9].

In 1980, the role of $s \rightarrow d$ transitions was reanalyzed once more. Scadron^[44,45] concentrated again on transitions in which no gluons were emitted from the $s - d$

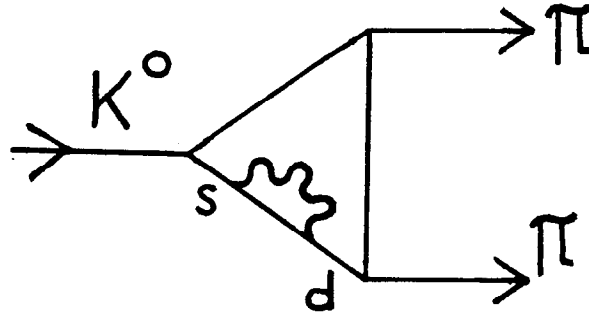


Fig. A4. One of diagrams for $K^0 \rightarrow \pi\pi$ decay, from Pascual and Tarrach article. The wavy line is a W boson.

quark line, and named them “tadpoles”. (Note that in “penguins” at least one virtual gluon connects $s - d$ line with another quark line, producing effectively a four-quark interaction. On the contrary, “tadpoles” correspond to pure two-body operators.) Scadron considered both diagrams and operators, and concluded that (i) diagrams (Fig. A5) are *not* suppressed, but of the order $G_F m_c^2$ in the hadron environment, and (ii) at least some of the two body operators $[\bar{d}(\mathbf{1}, \gamma_5, \not{\partial}, \not{\partial}\gamma_5)s]$, contrary to earlier claims, do survive in Hamiltonians. The argument is that a unitary rotation can only remove two operators (say, $[\bar{d}\mathbf{1}s]$ and $[\bar{d}\gamma_5 s]$) but thereafter, the rotation is fixed and no further redefinition of fields is allowed. Additionally, the wave function renormalization can not help to eliminate the remaining operators, when quarks are not free but confined in hadrons. With respect to diagrams, Scadron’s analysis of Fig. A5 was done in the renormalizable gauge, but again – as in Ref. 9 – without an inclusion of charged Higgs contributions.

Such an apparently incomplete procedure was met with some skepticism. In 1984, Chia^[43] published a systematic analysis of $s - d$ self-energy diagrams. His work confirms that in the field theory, after an addition of unphysical Higgs particles and the renormalization, the leading $G_F m_c^2$ terms in Fig. A5 are washed away, leaving only a highly suppressed and unimportant contributions. Note however that this result might not be relevant for Pascual and Tarrach^[9], and Scadron’s^[44,45]

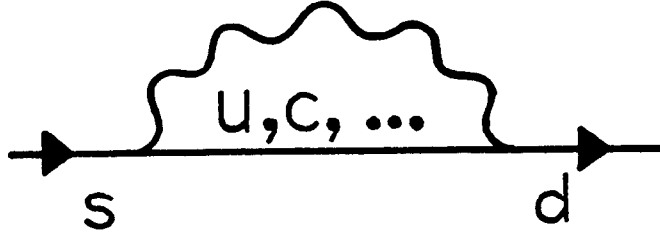


Fig. A5. An $s - d$ self-energy diagram.

works. The quarks in their approach were not current quarks, but quarks immersed in hadrons and already dressed by QCD. If so, no further renormalization was needed, and since unphysical particles are mainly required to complete the renormalization procedure, maybe indeed there was no need for Higgs diagrams in their analyses. This argument was to some degree substantiated in a recent article by Shabalin^[46]. He *did* take into account Higgs particles, and also added all possible gluon corrections along $s - d$ line in Fig. A5. A large enhancement, not present when QCD is turned off, was obtained. So, gluons acted as catalysts, speeding up the process, just as in Refs. 9 and 44 was supposed. However, according to Shabalin's calculation, the sum of all short distance corrections gives $G_F \ln m_c^2$ rather than $G_F m_c^2$ used in Refs. 9 and 44. Shabalin's work was carefully studied by Guberina, Peccei and Picek^[47]. They debated the procedure by which the QCD summation^[46] was performed. Generally, they found operators corresponding to the dressed diagram in Fig. A5, to mix with both gauge non-invariant operators and those disappearing by equation of motion. Thus such operators are beyond reach of the usual renormalization group analysis, and the summation of leading log terms is probably not possible. Guberina *et al.*^[47] also stressed that in the chiral perturbation theory, $K \rightarrow$ vacuum matrix elements of all two-body $[\bar{d}s]$ operators are suppressed. This would be bad news for "tadpole" operators in conventional approaches: physical amplitudes are often related just to these matrix elements.

The use of perturbative QCD in studies of kaon decays has lost some of its

popularity in recent years. At the same time, Monte Carlo simulations on discrete lattices gained credibility. Non-perturbative contributions to K decay amplitudes are usually deduced from studies of matrix elements of weak Hamiltonian on a lattice. It is interesting that even in lattice simulations, the direct $s \rightarrow d$ transitions seem to play a significant role. They are represented by the so-called “eye” graphs (See *e.g.* Bernard *et al.*^[48], and also Ref. 49). It remains to be seen whether this will be confirmed when more reliable calculations, with bigger lattices and a direct evaluation of amplitudes (and not through the use of PCAC) become possible^[50]. Confronted with many uncertainties in determination of higher order (both long and short) QCD contributions to $s \rightarrow d$ transitions of confined quarks, the present author^[6-8] proposed in 1985 an inclusion of these transitions into wave functions of K and π . The resulting nonlocal “anomalous vertices” were characterized by unusual flavor structure: in addition to u and \bar{s} quarks, u and \bar{d} pair was also present in K^+ , *etc.* The idea is further expanded in this article.

In many other works $s \rightarrow d$ transitions were analysed or referred to, either in terms of diagrams or in terms of operators. Let me mention just a few. Ahmed and Ross^[51] presented an early analysis of $[\bar{d}s]$ operators. Tadić and collaborators^[52], and the Amherst group^[53], thoroughly studied the role of penguin operators in explanation of the $\Delta I = 1/2$ rule. Gilman and Wise^[54], and Guberina and Peccei^[55], analysed penguin contributions to CP-violation. Chau^[56] parametrized all two-body K decays in terms of several generic diagrams, reserving a prominent role for those with $s \rightarrow d$ transitions. For a follow-up of Scadron’s work see Ref. 57. Eeg^[58] used Shabalin’s dressed self-energy diagrams^[46] in study of some rare K decays.

Not all the explanations of the $\Delta I = 1/2$ rule in K decays rely on $s \rightarrow d$ transitions (see *e.g.*, Stech^[59], Preparata *et al.*^[60,61], and Terasaki^[62]). Still, these direct transitions provide one of the most elegant and simple solutions to the long-standing problem. Maybe one day we shall be able to calculate exactly the effect of such transitions. Or, if this turns out to be impossible, we still might benefit from the concept by having a better qualitative description, or by introducing a more suitable parametrization. The idea has been with us too long to be taken

lightly. In Gell-Mann's^[63] words, "... we should really either bury this thing, or else make use of it." The advice was given in 1958, when the concept of neutral, flavor changing direct transitions was only in diapers, but remains equally valid and actual today.

Appendix B : Alternative Model for Anomalous Vertices

I have repeated all the calculations mentioned in the main text in an alternative model. The goal of that study was to learn something about the model-dependency. In the alternative model (“Model B”), the probability distribution for anomalous vertices has the following form (compare to Eq. (4)):

$$\tilde{H}_{\mathcal{M}}^{\text{B}}(k, P) = \frac{1}{\pi^3} \frac{G_{\text{FSC}}}{\sqrt{2}} \beta_{\mathcal{M}} M_{\mathcal{M}}^{2n-3} \left(k \mp \frac{P}{2} \right)^2 \frac{\not{P} (X^{\text{B}} + Y^{\text{B}} \gamma_5)}{(k^2 - \alpha_{\mathcal{M}} P^2)^n} . \quad (\text{B1})$$

Note that the power in the denominator is n , instead of $n + 1$ used in the Model A. Expressions (5) and (9) remain unchanged, and so do the rules for evaluation of diagrams. Although the difference might look as a minor one, values of loop integrals change considerably in some cases.

Consider first the anomalous part of the $\pi^+ \rightarrow \bar{\ell} \nu$ amplitude (Fig. 9). Instead of the expression in the second line of Eq. (14), one finds

$$(-)^n i c f_{\pi} P^{\mu} \left[\frac{G_{\text{FSC}}^2}{\sqrt{2}} M_{\pi}^2 (X^{\text{B}} + Y^{\text{B}}) \frac{\alpha_{\pi}}{\pi^3} \left(\frac{1}{4\alpha_{\pi}} - \frac{2}{n-3} \right) \right] . \quad (\text{B2})$$

Equation (16), for the amplitude $\tilde{A}(1)$ in $K^S \rightarrow \pi^+ \pi^-$ decay, becomes replaced by

$$\begin{aligned} \tilde{A}(1) &= \frac{G_{\text{FSC}}}{\sqrt{2}} \frac{1}{\pi^3} (\beta_K M_K^{2n-3}) (\beta_{\pi} M_{\pi}^{2n-3})^2 (-3) i^3 \int \frac{d^4 k}{(2\pi)^4} \\ &\frac{1}{\sqrt{2}} \left[\left(k + \frac{P}{2} \right)^2 - \left(k - \frac{P}{2} \right)^2 \right] \text{Tr} \left\{ \left(\not{k} + \frac{\not{P}}{2} - m_d \right) \frac{\not{P} (X^{\text{B}} + Y^{\text{B}} \gamma_5)}{B^n} \right. \\ &\left. \left(\not{k} - \frac{\not{P}}{2} - m_d \right) \frac{\not{S} \gamma_5}{C^n} \left(\not{k} + \frac{\not{S} - \not{R}}{2} - m_u \right) \frac{\not{R} \gamma_5}{D^n} \right\} . \end{aligned} \quad (\text{B3})$$

The remaining two amplitudes, Eq. (26), get changed in a similar way, leading to the total anomalous amplitude (compare to Eq. (27)),

$$(\tilde{A}_{+-}^S)_{\text{Model B}} = \frac{G_{\text{FSC}}}{\sqrt{2}} M_K^2 f_{\pi} X^{\text{B}} \cdot \tilde{I}^{\text{B}} . \quad (\text{B4})$$

With $n = 5$, one finds $\tilde{I}^{\text{B}} \rightarrow \tilde{I}_{(5)}^{\text{B}} = -0.97$. Therefore, in order to describe the

experimental value $\tilde{A}_{+-}^S \sim 376$ eV, one must choose $\tilde{X}_{(5)}^B \simeq -6.8$.

When the decay $K^+ \rightarrow \pi^+ \gamma_Y$ is considered, one finds that the amplitude A_{ANOM} becomes (compare to Eq. (30))

$$A_{\text{ANOM}}^\tau = \frac{G_{\text{Fsc}}}{\sqrt{2}} (\beta_K M_K^{2n-3}) (\beta_\pi M_\pi^{2n-3}) f Y^B (-3) \int \frac{d^4 k}{(2\pi)^4} \quad (B5)$$

$$\frac{1}{\pi^3} \left[\frac{C_u J^\tau(1) - C_d J^\tau(2) + C_u J^\tau(3) - C_s J^\tau(4)}{V^n U^n} \right]$$

This expression gives (with $n = 5$)

$$(A_{\text{ANOM}}^\tau)_{\text{Model B}} = +i \frac{G_{\text{Fsc}}}{\sqrt{2}} f f_\pi f_K [0.2114 Y_{(5)}^B] P^\tau + \dots \quad , \quad (B6)$$

and the branching ratio

$$B = 0.0537 [Y_{(5)}^B]^2 \frac{f^2}{m_Y^2} \times 10^{16} \text{ eV}^2 \quad . \quad (B7)$$

Whenever masses of quarks were required in calculations, in both Models A and B, the values

$$m_u = m_d = 0.010 \text{ GeV} \quad , \quad m_s = 0.150 \text{ GeV} \quad , \quad (B8)$$

were used. The other numerical constants, $G_{\text{F}} = 1.1664 \times 10^{-23} \text{ eV}^{-2}$, $s = 0.222$, $c = 0.975$, $M_K = 0.495 \text{ GeV}$, and $M_\pi = 0.140 \text{ GeV}$, have the standard values (see *e.g.*, the Particle Data brochure^[18]).

REFERENCES

1. See *e.g.*, the recent review, H.-Y. Cheng, *Status of the $\Delta I = 1/2$ Rule in Kaon Decays*, Indiana University Report IUHET-132 (1987), unpublished.
2. M. K. Gaillard and B. W. Lee, *Phys. Rev. Lett.* **33**, 108 (1974)
3. G. Altarelli and L. Maiani, *Phys. Lett.* **52B**, 351 (1974)
4. K. G. Wilson, *Phys. Rev.* **179**, 1499 (1969)
5. H. Galić, *Phys. Rev.* **D24**, 3000 (1981)
6. H. Galić, *Z. Phys.* **C29**, 519 (1985)
7. H. Galić, *Fizika* **17**, 501 (1985)
8. H. Galić, *Phys. Rev.* **D31**, 2363 (1985)
9. P. Pascual and R. Tarrach, *Phys. Lett.* **87B**, 64 (1979)
10. C. J. Gilmour, *Z. Phys.* **C18**, 163 (1983)
11. S. Oneda, J. C. Pati, and B. Sakita, *Phys. Rev.* **119**, 482 (1960)
12. R. E. Marshak, Riazuddin, and C. P. Ryan, *Theory of Weak Interactions in Particle Physics*, Wiley, New York (1969)
13. H. Pietschmann *Weak Interactions — Formulae, Results, and Derivations*, Springer, Wien (1974), Addendum 7
14. E. D. Commins and P. H. Bucksbaum, *Weak Interactions of Leptons and Quarks*, Cambridge University Press, Cambridge (1983), Section 6
15. See *e.g.* the amplitude (B2), in M. Milošević, J. Trampetić, and D. Tadić, *Nucl. Phys.* **B187**, 514 (1981). When QCD coupling constant is set to zero, one recovers the result (24).
16. For a discussion, see *e.g.*, F. Hussain and M. D. Scadron, *Phys. Rev.* **D30**, 1492 (1984)

17. Recently, I learned that the same factor of 2 discrepancy appeared in lattice estimates of the $K^+ \rightarrow \pi^+\pi^0$ amplitude. See *e.g.*, C. Bernard, T. Draper, G. Hockney, and A. Soni, Nucl. Phys. B (Proc. Suppl.) 4, 483 (1988), and M. B. Gavela *et al.*, Nucl. Phys. B306, 677 (1988). Are we maybe facing another “crisis” in understanding of K decays?
18. Review of Particle Properties, Phys. Lett. 170B, 1 (1986)
19. E. Fischbach, D. Sudarsky, A. Szafer, C. Talmadge, and S. H. Aronson, Phys. Rev. Lett. 56, 3 (1986); 56, 1427(E) (1986)
20. S. C. Holding, F. D. Stacey, and G. J. Tuck, Phys. Rev. D33, 3487 (1986)
21. A. T. Hsui, Science 237, 881 (1987)
22. P. E. Boynton, D. Crosby, P. Ekstrom, and A. Szumilo, Phys. Rev. Lett. 59, 1385 (1987)
23. D. H. Eckhardt, C. Jekeli, A. R. Lazarewicz, A. J. Romaides, and R. W. Sands, Phys. Rev. Lett. 60, 2567 (1988)
24. See also the recent review article, E. Fischbach and C. Talmadge, *The Fifth Force: An Introduction to Current Research* (presented at 7th Moriond Workshop on Searches for New and Exotic Phenomena, Les Arcs, 1988), Purdue University Report, PURD-TH-88-6 (1988), unpublished
25. It also must be mentioned that in several experiments no physically significant deviation was observed. For a list of these experiments, see *e.g.* Ref. 24.
26. F. D. Stacey *et al.*, Rev. Mod. Phys. 59, 157 (1987)
27. C. Talmadge and E. Fischbach, *Searching for the Source of the Fifth Force* (presented at Erice School of Cosmology and Gravitation, 1987), Purdue University Report, PURD-TH-87-19 (1987), unpublished

28. C. Talmadge and E. Fischbach, *Phenomenological Description of the Fifth Force* (presented at 7th Moriond Workshop on Searches for New and Exotic Phenomena, Les Arcs, 1988), Purdue University Report, PURD-TH-88-7 (1988), unpublished
29. E. Fischbach, D. Sudarsky, A. Szafer, C. Talmadge, and S. H. Aronson, *Ann. Phys. (N.Y.)* 182, 1 (1988)
30. Y. Asano *et al.*, *Phys. Lett.* 107B, 159 (1981); 113B, 195 (1982)
31. BNL Experiment 787
32. M. Suzuki, *Phys. Rev. Lett.* 56, 1339 (1986)
33. S. H. Aronson, H.-Y. Cheng, E. Fischbach, and W. Haxton, *Phys. Rev. Lett.* 56, 1342 (1986); 56, 2334 (E) (1986)
34. C. Bouchiat and J. Iliopoulos, *Phys. Lett.* 169B, 447 (1986)
35. M. Lusignoli and A. Pugliese, *Phys. Lett.* 171B, 468 (1986)
36. Recently, another decay channel, namely $K^0 \rightarrow \pi^+\pi^-\gamma\gamma$, was studied by J. Trampetić *et al.*, Purdue University Report (1988), unpublished. Authors found that the analysis of this mode was much less dependent on details of calculation, than in the mode $K^+ \rightarrow \pi^+\gamma\gamma$.
37. See *e.g.*, S. Aronson, E. Fischbach, D. Sudarsky, and C. Talmadge, *The Compatibility of Gravity and Kaon Results in the Search for New Forces*, Report BNL-41475 (1988), unpublished
38. C. Bernard, A. Soni, and T. Draper, *Phys. Rev. D* 36, 3224 (1987)
39. S. R. Sharpe, A. Patel, R. Gupta, G. Guralnik, and G. W. Kilcup, *Nucl. Phys. B* 286, 253 (1987)
40. L. Maiani, G. Martinelli, G. Rossi, and M. Testa, *Nucl. Phys. B* 289, 505 (1987)
41. S. L. Glashow, J. Iliopoulos, and L. Maiani, *Phys. Rev. D* 2, 1285 (1970)

42. M. A. Shifman, A. I. Vainshtein, and V. I. Zakharov, Nucl. Phys. B120, 316 (1977)
43. S. P. Chia, Phys. Lett. 147B, 361 (1984)
44. M. D. Scadron, Phys. Lett. 95B, 123 (1980)
45. See also B. H. J. McKellar and M. D. Scadron, Phys. Rev. D27, 157 (1983)
46. E. P. Shabalin, ITEP Report 86-112 (1986), unpublished
47. B. Guberina, R. D. Peccei, and I. Picek, Phys. Lett. 188B, 258 (1987)
48. C. Bernard, T. Draper, G. Hockney, A. M. Rushton, and A. Soni, Phys. Rev. Lett. 55, 2770 (1985)
49. C. Bernard, A. El-Khadra, and A. Soni, *Weak Decays on the Lattice: Current Status and Future Prospects* (presented at Ringberg Workshop on Hadronic Matrix Elements and Weak Decays, 1988), UCLA Report UCLA/88/TEP/31 (1988), unpublished
50. For some preliminary results of a “direct” calculation see *e.g.* Bernard *et al.* in Ref. 49. Although PCAC was not used in Ref. 49, the work still rely heavily on the standard, four-quark, effective weak Hamiltonian.
51. M. A. Ahmed and G. G. Ross, Phys. Lett. 61B, 287 (1976)
52. H. Galić, D. Tadić, and J. Trampetić, Nucl. Phys. B158, 306 (1979)
53. J. F. Donoghue, E. Golowich, W. A. Ponce, and B. R. Holstein, Phys. Rev. D21, 186 (1980)
54. F. J. Gilman and M. B. Wise, Phys. Rev. D20, 2392 (1979)
55. B. Guberina and R. D. Peccei, Nucl. Phys. B163, 289 (1980)
56. L.-L. Chau, Phys. Reports 95 (1983) 1
57. M. D. Scadron and S. R. Choudhury, *Simple Theory of Nonleptonic Kaon Decays*, ICTP Report IC/87/180 (1987), unpublished
58. J. O. Eeg, Phys. Lett. 196B, 87 (1987)

59. B. Stech, Phys. Rev. D36, 975 (1987)
60. G. Nardulli, G. Preparata, and D. Rotondi, Phys. Rev. D27, 557 (1983)
61. G. Preparata, in *Hadronic Physics at Intermediate Energies II*, (Proceedings of Winter School of Hadronic Physics, Folgaria, Italy, 1987), edited by T. Bressani *et al.*, North Holland, Amsterdam (1987)
62. K. Terasaki, S. Oneda, and T. Tanuma, Phys. Rev. D29, 456 (1984)
63. M. Gell-Mann, in *1958 Annual International Conference on High Energy Physics at CERN, (Proceedings)*, edited by B. Ferretti, CERN, Geneva (1958), p. 261 (Discussion)